Georg Greil, BSc

Process development for calcination of PTC materials with a rotary tube kiln

Master's Thesis

zur Erlangung des akademischen Grades

Diplom Ingenieur

eingereicht an der

Technischen Universität Graz

Betreuer

Univ.-Prof. Dipl.-Phys. Dr.rer.nat. Roland Würschum

Institut für Materialphysik

In Kooperation mit EPCOS OHG, a TDK Group company

Graz, Mai 2017

Statutory Declaration

I declare that I have authored this thesis independently, that I have not used other than the declared sources/resources, and that I have explicitly marked all material which has been quoted either literally or by content from the used sources.

Graz, _____ _____

Date Signature

Eidesstattliche Erklärung[1]

Ich erkläre an Eides statt, dass ich die vorliegende Arbeit selbstständig verfasst, andere als die angegebenen Quellen/Hilfsmittel nicht benutzt, und die den benutzten Quellen wörtlich und inhaltlich entnommenen Stellen als solche kenntlich gemacht habe.

Graz, am _____ _____

Datum Unterschrift

[1] Beschluss der Curricula-Kommission für Bachelor-, Master- und Diplomstudien vom 10.11.2008; Genehmigung des Senates am 1.12.2008

Kurzfassung

Materialien mit positivem Temperaturkoeffizienten (PTC) des elektrischen Widerstands finden in zahlreichen Gebieten der Technik Anwendung. Für die teils sehr unterschiedlichen Einsatzgebiete müssen diese temperaturabhängigen Bauteile präzise mit den gewünschten Eigenschaften hergestellt werden können. Dies geschieht einerseits über Materialzusammensetzung und andererseits durch den Einfluss des Produktionsprozesses. Die vorliegende Arbeit wird in Kooperation mit EPCOS OHG erstellt und untersucht den Einsatz einer neuen Möglichkeit für den Herstellungsschritt der Kalzination in der PTC-Produktion am Standort Deutschlandsberg. Es wird der Einsatz eines Drehrohrofens anstelle des aktuell verwendeten Durchschubofens untersucht. Dabei liegt der Fokus auf einer Mischung von Ausgangsmaterialien, die für die Produktion von Motorstart-Bauteilen verwendet wird. Das Ziel dieser Arbeit ist ein Kalzinationsverfahren zu entwickeln, das die Produktion von PTC Bauteilen erlaubt, deren Eigenschaften genauer geregelt werden können als im bisher verwendeten Prozess. Eine Effizienzsteigerung im Hinblick auf Energieverbrauch und Durchsatz kann erwartet werden. Im ersten Schritt werden dabei Parameter definiert und Werte festgelegt. Diese Werte werden in Langzeitversuchen auf Stabilität und Reproduzierbarkeit untersucht. Im nächsten Schritt wird ein statistischer Versuchsplan erstellt. Dieser liefert die Grundlage zur Erstellung eines Modells, das den Einfluss der einzelnen Parameter auf den Prozess beschreibt. Dieses Modell kann genutzt werden, um den Produktionsprozess genau zu regeln und somit die Qualität des Produkts zu steigern.

Abstract

Materials with a positive temperature coefficient (PTC) of the electrical resistance find various applications in technology.
For the very diverse applications of the temperature sensitive parts a precise production process is required to achieve the desired features. This is accomplished by material composition on the one hand and by process control on the other hand.
This thesis is written in cooperation with EPCOS OHG and targets to evaluate and install a new process step in PTC production. This step is the calcination of material at the PTC facility in Deutschlandsberg. The application of a rotary tube kiln replacing the pusher kiln in use is investigated. The main focus lies on a material mixture used for production of motor start devices. The goal of this thesis is to develop a calcination process for production of PTC devices with improved control over powder properties and PTC features. Also an increase in efficiency in terms of energy consumption and performance is expected. The first step is defining parameters and their values for replacing the pusher kiln process. The process is being investigated in long term experiments to show reproducibility and stability. In the final step a statistical series of experiments is designed which lays the basis for a descriptive model of the influence of parameters on the process. This model is used for process control and an improvement of the product quality.

Acknowledgements

I would like to sincerely thank the following people who supported me in my research and who contributed to the completion of this thesis:

Univ.-Prof. Dr. Roland Würschum, Institute of Materials Physics, TU Graz
For support with literature, help improving this written work and enabling the cooperation with EPCOS OHG.

Dipl.Ing. Jürgen Hermsdörfer, EPCOS OHG
For all hard work, highly competent and friendly supervision. For assistance with all matters, help where needed and for letting me work independently where possible.

EPCOS OHG and all staff at the facility in Deutschlandsberg
For giving me the possibility to write this work and gather experience in a company surrounding. For all support in machine and material handling, measurements and for their open and friendly minds.

All my family
Especially my beloved family in Graz for great support and cheering up in all situations. My parents and siblings for great motivation and advice.

Glossary

Acronyms and their explanations are given here.

- **DoEx**: ***D**esign **o**f **Ex**periments* - A statistical approach on planning experiments.
- **PTC**: ***P**ositive **t**emperature **c**oefficient resistor* - An electric component with temperature sensitive resistance.
- **APM**: ***A**dvanced **P**ower **M**etal* - A Chrome, Iron, Aluminium metal alloy. One tube used with the rotary tube kiln is made from this material.
- **C610**: A mullite ceramic used for various technical applications. One tube used with the rotary tube kiln is made from this material.
- **rpm**: ***R**ounds **p**er **m**inute* - Unit describing rotary speeds
- T_{cal}: *Calcination temperature* - The temperature setting for calcination in experiments (process parameter)
- T: *Temperature* - In this work given as °C
- R: *Electrical resistance* - Measured with an Ohmmeter
- I_t: *Tube inclination* - Inclination of the rotary tube kiln tube in °
- v_t: *Tube driver rotary speed* - Rotary speed of rotary tube kiln tube in rpm
- v_f: *Feeding mechanism driver speed* - Given in rpm
- q_t: *Material throughput* - Material output per time in $\mathrm{kg\,h^{-1}}$
- R_{25}: *Room temperature resistance* - Electrical resistance at room temperature of 25 °C, measured in Ω after first sintering
- T_{Rmin}: *Temperature at minimum electrical resistance* - Temperature at point of minimal resistance in measured R-T characteristics, measured in °C after final sintering
- T_{ref}, (T_b): *Reference temperature* - Temperature at which resistance reached twice minimum resistance, measured in °C after final sintering

Contents

1 Introduction

This chapter describes the motivation for this work and introduces the surroundings.

All experiments were conducted for EPCOS OHG at the production facility in Deutschlandsberg. EPCOS OHG is a TDK Group company. The facility houses a PTC production line with main focus on calcination.

Positive temperature coefficient (PTC) resistors are temperature sensitive electrical resistors. They find application in various systems as protective devices, heaters, current limiters, gas flow sensors and many more. A very big emerging market for PTC devices is electro-mobility as heating elements are needed for electric driven vehicles in contrast to combustion engines where heat generation is inherent. [1]
As PTCs are ceramic elements their production requires special facilities, careful raw material handling and a good process control. The PTC effect is not observed in single crystal materials and has to be seen as a grain boundary effect. [7]
The growth of grain boundaries is the main factor determining the final properties of the PTC resistors. Therefore the manufacturing process influences properties strongly, in addition to the composition of the raw material. This work investigates the possibility of replacing the standard pusher kiln process by a rotary tube kiln and targets to find possibilities for process control via a design of experiments (DoEx). Materials characterization includes lattice distortion, specific surface area, and various powder properties.

Barium titanate is the most common PTC resistor material. Dopants are added to the raw material mixture to adjust electrical properties. The critical temperature, which also defines the working area of the final product can be shifted by adding lead or

strontium to a barium titanate mass (chapter 2). This also influences the calcination temperature.

Due to the great number of possibilities in raw material composition names are given for defined recipes and are internal standards of EPCOS OHG. The most used PTC mass in this work is named "EB271". It is a barium carbonate and titan oxide mixture containing also lead oxide of about 17 %. It is designed for the production of motor start PTCs.

The aim of this work is to find the influence of rotary tube kiln working parameters on the calcination process and the final product. The prerequisite is that parameters are found for which the rotary tube kiln process produces comparable calcined powder to the standard pusher kiln process. A design of experiments is then used to determine possibilities for process control which allow to improve the quality of calcination.

In the standard pusher kiln process capsules of Cordierite are filled manually with a raw material mixture. The capsules are closed with lids which are not gas tight. The capsules are moved into a pusher kiln and run through a heating up, firing and cool down stage. The process takes about 20 h per capsule. A schematic for the process can be found in Figure 1.1.

For a uniform calcination the capsules can only contain a limited amount of powder due to heat transfer and temperature gradients inside the capsule. This process, as used in production at EPCOS OHG in Deutschlandsberg, can produce about $40\,\mathrm{kg\,h^{-1}}$.

A rotary tube kiln offers the possibility to calcine powder in a continuous process. The raw material mixture can be fed to the tube by a spiral conveyor and calcined powder can be collected in containers at the tube end. A more uniform calcination of powder and higher quality can be expected as all particles experience the same conditions by constant revolving of material which ensures homogeneity. A schematic comparison of the rotary tube to pusher kiln calcination can be found in Figure 1.1.

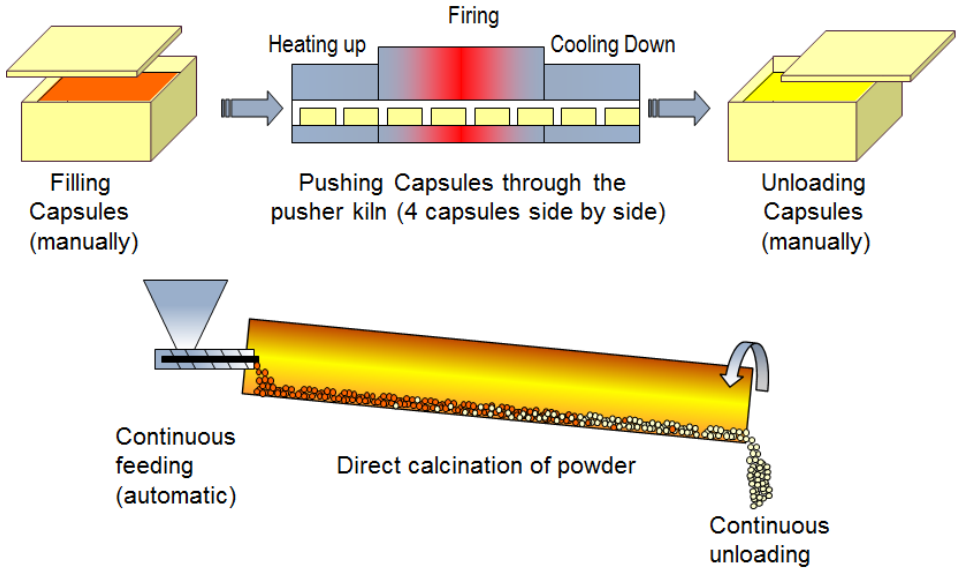

Figure 1.1: Schematic drawing of pusher kiln and rotary tube kiln process. [TDK]

One big advantage of the rotary tube kiln process is that no saggers (capsules) are needed. This results in easier handling as capsules need to be filled and emptied manually. The direct calcination also consumes less power and a more environmentally friendly process is possible.

The potential advantages of a rotary tube kiln over the pusher kiln process are as follows:

- Uniform calcination
- Less variation of powder properties
- Higher quality products
- Enable new possibility for process control
- Lower energy consumption
- Automation possible

The calcined powder is investigated by X-ray diffractometry to measure the tetragonal lattice distortion and by B.E.T. analysis to determine the specific surface area. After milling and spray drying the powder is investigated by X-ray fluorescence analysis and ICP spectroscopy to find possible contaminations. Powder properties are also determined for the calcined powder. Electrical measurements are conducted after sintering.

2 Positive temperature coefficient resistors

The main aspect of this thesis is the production of PTC resistors. Therefore a short overview of the basic principles and properties of these components is given in this chapter in section 2.1 and section 2.2. The main steps in PTC fabrication are outlined in section 2.3. A short description of the used material for PTC production, barium titanate, is given in section 2.4.

2.1 Typical PTC applications

Positive temperature coefficient (PTC) resistors are electrical resistors with positive (rising) resistance characteristics over a certain region of temperature which is the working area. (see Figure 2.1)

This temperature sensibility offers various application possibilities, such as overheating protection in electrical applications, start control for motors and temperature measurements. This work mainly focuses on a raw material mixture designed for production of motor start PTC devices.

PTC devices can also be used for the detection of the flow rate of gases or for measuring icing conditions on a helicopter blade or the height of liquid in a tank. Another application is the use as a self-regulating heating element in a hair dryer or the emerging market of electrical vehicles. For these applications an electric working point (voltage-current) is chosen with thermal equilibrium temperature close to the

temperature of the steeply rising resistance. E.g. when a fuel tank is empty a certain thermal equilibrium is established. A change of heat dissipation (e.g. fuel tank is filled) causes a change in voltage-current characteristics (thermal equilibrium at lower temperature) which allows detection (change of resistance). [7, 3]

2.2 PTC properties

PTC resistors are electrical components that change their resistance with temperature. This phenomenon is strongest close to the critical temperature, which is connected to the ferroelectric Curie temperature for barium titanate. [7]

A schematic resistance (R) - temperature (T) characteristics for PTCs is shown in Figure 2.1. The material shows in the region (AB) and at higher temperatures (CD) a negative resistivity- temperature characteristics as common for semiconductors, while between these (BC) there is steep rise of resistance of several orders of magnitude. This rise (BC) is caused by a grain boundary effect rather than charge carriers (AB,CD).

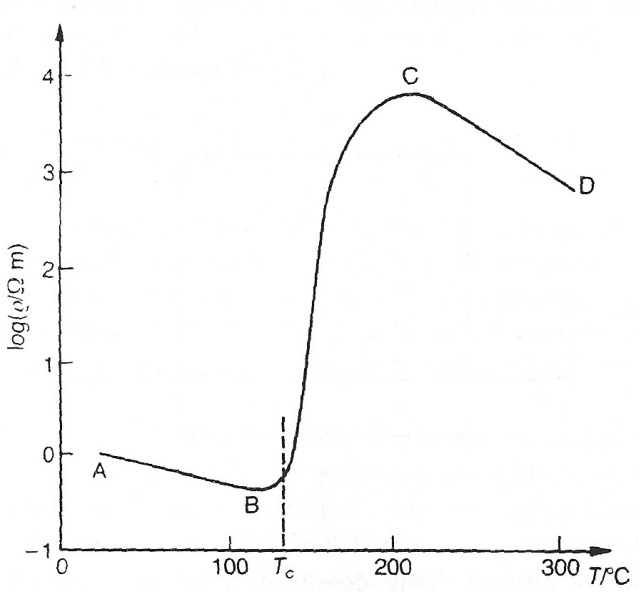

Figure 2.1: Typical resistance temperature characteristics of PTC thermistor. B to C - typical working area, T_c - critical temperature. [7], page 147

The PTC effect occurs in specially doped and processed barium titanate. Because the effect is not observed in the single-crystal form of the material its cause must be

assumed to lie in processes associated with grain boundaries.[7, 3]

An electrical double layer is formed at the grain boundaries by electron acceptor states and nearby ionized donor stated. The PTC effect is seen to have its origins in the resistance of the grain boundary region, which increases exponentially with temperature (T) above the ferroelectric-paraelectric transition temperature. At low temperatures the potential barriers at a fraction of the grain boundaries are reduced by spontaneous polarization of the crystal. These low resistance sites dominate the overall resistance. The polarization effect vanishes above the critical temperature and a steep rise of resistance can be observed. The relation of R with T is sketched in Equation 2.1 and can be found in more detail in [13].

$$\frac{1}{R} \propto \sigma \propto \exp\left(-\frac{\Phi_b}{kT}\right) \tag{2.1}$$

$$\Phi_b \propto \frac{1}{\epsilon} \tag{2.2}$$

$$\epsilon \propto \frac{1}{T - T_c} \tag{2.3}$$

$$R \propto \exp\left(1 - \frac{T_c}{T}\right) \propto \exp\left(-\frac{T_c}{T}\right) \propto \exp\left(\frac{T}{T_c}\right) \tag{2.4}$$

- R - Electrical resistance
- σ - Electrical conductivity
- Φ_b - Potential barrier height
- k - Boltzmann constant
- T - Temperature
- ϵ - Permittivity
- T_c - Curie temperature

The critical temperature T_{crit} of barium titanate can be shifted very easily by altering the composition. Replacing Barium in $BaTiO_3$ by strontium lowers the critical temperature and replacement with lead raises it, see Figure 2.2. Therefore it is simple to prepare resistors with T_{crit} of about $-100\,^{\circ}\mathrm{C}$ to $250\,^{\circ}\mathrm{C}$, although the highest temperature coefficients are found in barium titanate compositions without major quantities of substituents. [7]

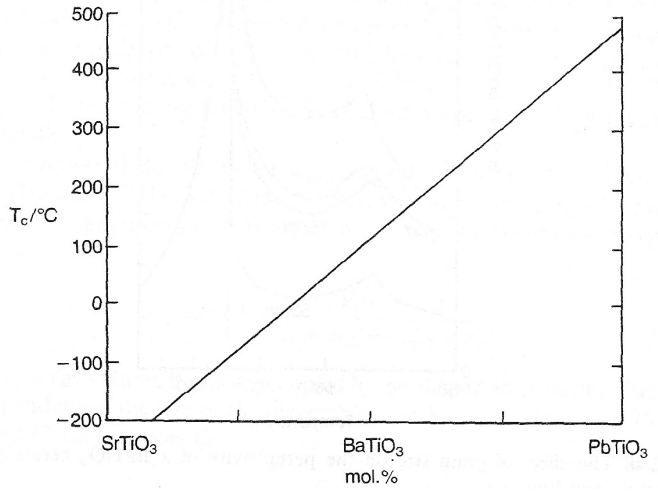

Figure 2.2: The effect on the critical temperature caused by substitution of barium for either strontium or lead in $BaTiO_3$. [7], page 77

2.2.1 Characterization

A measurement of a temperature resistance curve can be characterized as shown in schematic Figure 2.3. More information is provided by TDK / EPCOS OHG [1].

Important parameters are:

- $R25^*$, the resistance at 25 °C
- T_{min} (also T_{Rmin}) the temperature of minimum resistance
- T_{ref} (or T_B), the temperature where the resistance equals twice the value at T_{min}.

These parameters are used to qualify the produced PTC resistors and can also be used as process control targets.

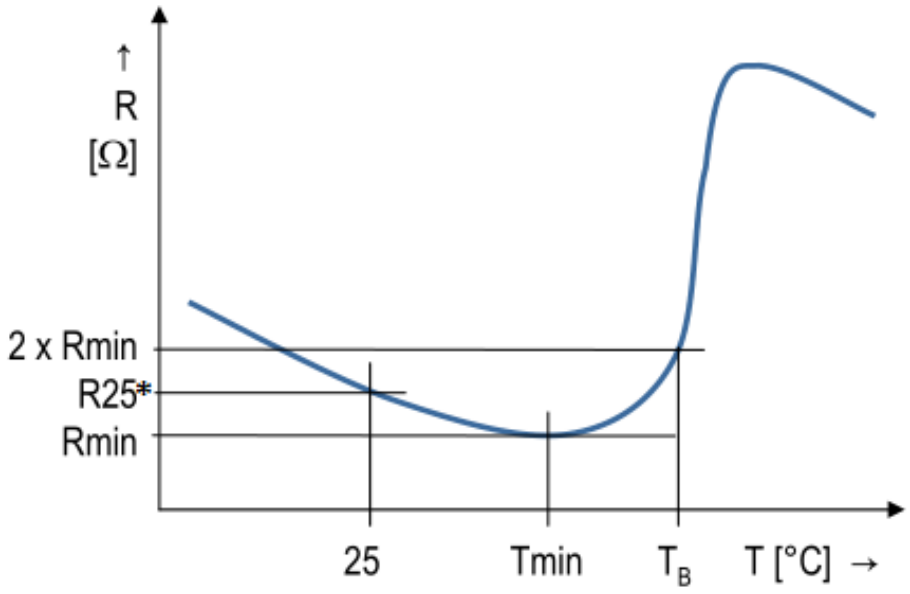

Figure 2.3: Schematic drawing of resistance temperature curve of a PTC resistor. Important characterization points are marked. [TDK]

2.3 Fabrication of PTC resistors

A good overview of the fabrication of PTC resistors is found in [7] and [3].

The basic composition for $BaTiO_3$ is usually derived from oxides or carbonates, such as $BaCO_3$, $SrCO_3$, TiO_2, PbO_2 etc., which are mixed in a ball-mill using mullite or agate balls and deionized water. The mix is dried and calcined (about 1000 °C) (see chapter 3). The calcined powder is ball-milled to a size of about 1 µm. At this stage other dopants and binders can be added. The slurry is then granulated, usually by spray drying, whereupon it is ready for pressing into discs. Sintering at about 1350 °C in air and the subsequent cooling stages have to be carefully controlled since this is when the barrier-layer characteristics are established. After the sintering stage, electrodes are applied, usually by painting or spraying on specially adapted silver paint.

2.4 Barium titanate

Barium titanate ($BaTiO_3$) shows the same structure as perovskite ($CaTiO_3$) and is therefore referred to have "perovskite structure". Above the critical temperature the unit cell is cubic as in Figure 2.4.

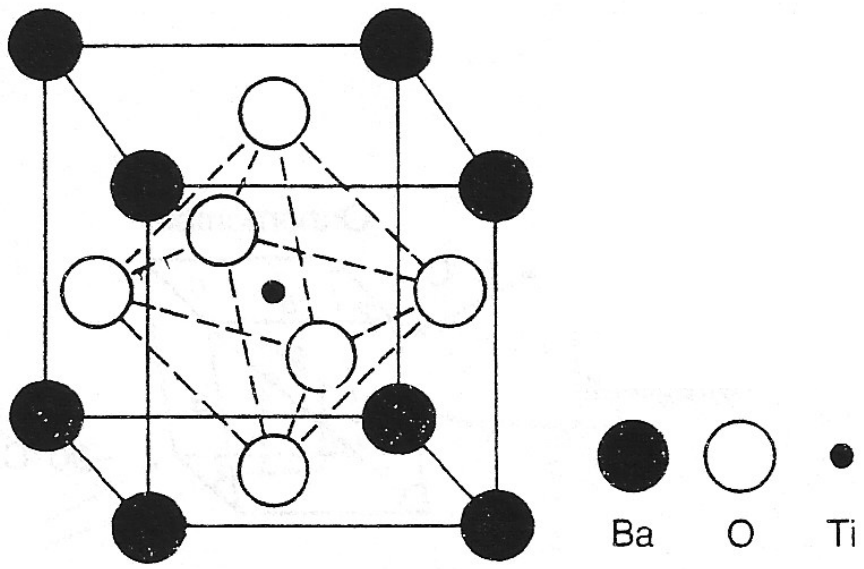

Figure 2.4: The unit cell of $BaTiO_3$ in cubic form (perovskite). Taken from [7]

Below this temperature the structure is distorted to the tetragonal form and shows a dipole moment along the c direction, see Figure 2.5. [7]

Barium titanate is the first ceramic in which ferroelectricity was observed and can be used as a model to describe the phenomenon in microstructure. A spontaneous polarization is observed in the material. It is energetically favourable for the ions to move in the same direction in the cubic-tetragonal transformation. The potential energy of the Ti^{4+} in terms of displacement takes the form of two wells and an external field can enable the ion to overcome the barrier between the two wells. The direction of the polarity is reversed. This also affects neighbouring ions and eventually a whole region can be influenced by the field. There is also a mechanism for 90° changes of polarity. In order of minimizing energy, regions of the same polarity are formed (caused by spontaneous polarization) which are called domains. This ferroelectric behaviour

influences the potential barrier in grain boundaries and therefore contributes to the PTC effect. [7]

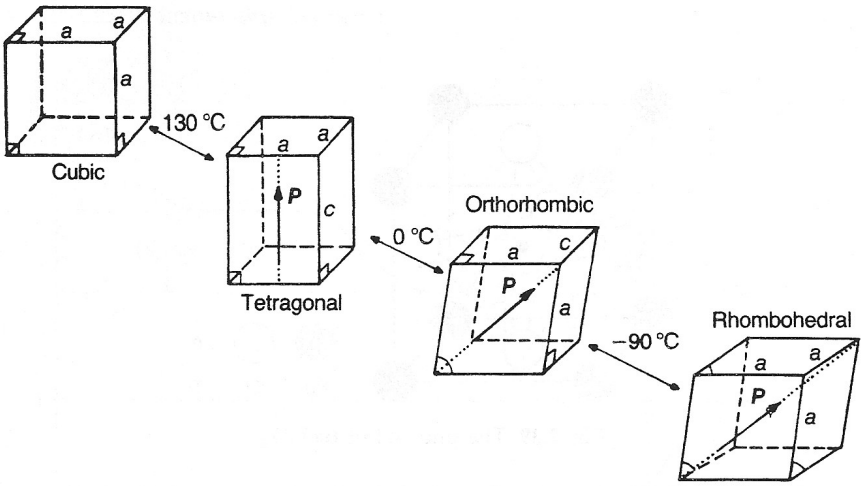

Figure 2.5: The unit cell structures of $BaTiO_3$.
Tetragonal form with a dipole moment in the c direction.
Orthorombic with the polar axis parallel to a face diagonal.
Rhombohedral with the polar axis along a body diagonal. Taken from [7]

The final product can be seen in Figure 2.6

Figure 2.6: Picture of a PTC resistor manufactured by EPCOS.

3 Calcination of barium titanate

This chapter introduces the mechanical and chemical steps in formation of barium titanate ($BaTiO_3$).

3.1 Calcination methods

Figure 3.1: Rotary tube kiln, model Nabertherm RSR

" Calcination causes the constituents to interact by interdiffusion of their ions and so reduces the extent of the diffusion that must occur during sintering in order to obtain a homogeneous body. It can therefore be considered to be part of the mixing process. " [7]

This means that most of the barium titanate formation occurs in the calcination step and assists further processing. This also influences the final electrical features as well as powder properties important for production steps.

During calcination the required final phases may not be completely formed, therefore, chemical gradients remain which may assist sintering. The main requirement is that calcination should yield a very homogeneous product, which can be achieved by different methods.

One calcination possibility is placing the mixed raw materials in saggers (capsules for calcination), which are put in or pushed trough a heating. The saggers need to be closed if the raw material contains any volatile constituent, such as lead oxide but need to allow gases formed during calcination to escape. As thermal conductivity of powders is rather low only a limited volume of powder can be treated with uniform temperature in one sagger. A schematic drawing of a pusher kiln and a rotary tube kiln can be found in Figure 1.1.

Another possibility for calcination is offered in a continuous process by a rotary tube kiln. It consists of a slowly rotating tube inclined to the horizontal so that material moves through the heated zone in desired conditions and speed. Heat can be supplied from combustion inside the tube or by heating of the tube from outside (indirect). A laboratory sized rotary tube kiln is shown in Figure 3.1.

The calcined material can be partly sintered in the process and needs to be milled to enable further processing such as shaping. A desired particle size can be achieved by milling after the calcination process and also assists further processing.

3.2 Formation of barium titanate

Lead, strontium and other elements can be introduced in the crystal lattice occupying the sites of barium in the perovskite structure. This leads to a shifted critical temperature and also strongly influences the needed calcination temperatures. The following section discusses only barium titanate without additions. (see Figure 2.2) [7]

Figure 3.2 shows the phases of the materials which occur for different firing temperatures. Starting from the raw materials $BaCO_3$ and TiO_2 the formation of Ba_2TiO_4 is observed from about 800 °C. At higher temperatures the formation of $BaTiO_3$ starts, but only at very high temperatures of 1200 °C it is the only remaining phase and the calcination is finished.

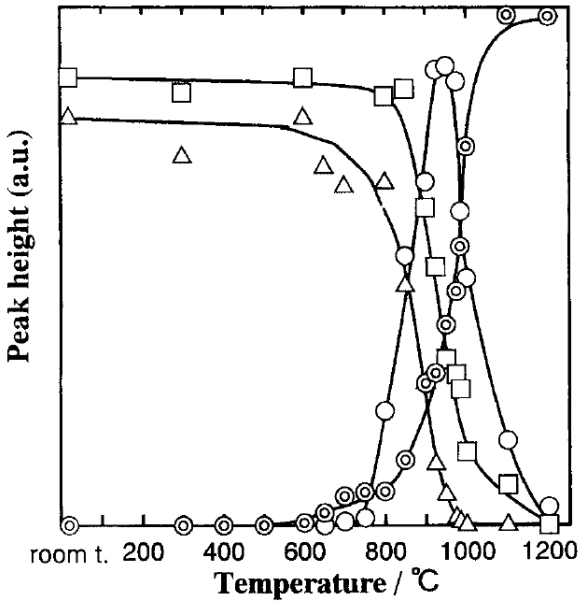

Fig. 2. Relation between XRD's peak heights of specimens fired and firing temperatures (peak heights of the strongest diffraction ray were used).
△ $BaCO_3$, □ TiO_2, ○ Ba_2TiO_4, ◎ $BaTiO_3$

Figure 3.2: Phase composition for different temperatures during the formation of barium titanate. Taken from [9]

The formation of barium titanate is divided into three steps as found in [9].

- $BaCO_3 + TiO_2 \rightarrow BaTiO_3 + CO_2$
- $BaTiO_3 + BaCO_3 \rightarrow Ba_2TiO_4 + CO_2$
- $Ba_2TiO_4 + TiO_2 \rightarrow 2BaTiO_3$

Barium carbonate $BaCO_3$ and titanium oxide TiO_2 react only on the surfaces to barium titanate $BaTiO_3$. Barium orthotitanate Ba_2TiO_4 is then formed at higher firing temperatures. Only at even higher temperatures $BaTiO_3$ is the only remaining component of the reaction (see Figure 3.3). As one can see carbon dioxide is formed in the process and needs to be able to escape the process site.

A schematic evolution of the particles which also shows the formation of pores in the material can be found in Figure 3.3. From about 600 °C the first $BaTiO_3$ is formed on the surface between $BaCO_3$ and TiO_2 (*b*). At the inside of the thin $BaTiO_3$ layer excess *Ba* forms Ba_2TiO_4 (*c*). Barium ions move to the TiO_2 particles (forming $BaTiO_3$ there) starting from $BaCO_3$ moving over Ba_2TiO_4 and $BaTiO_3$ layers. As long as $BaCO_3$ is present Ba_2TiO_4 is formed at the inside of the $BaTiO_3$ parallel to the formation of $BaTiO_3$.

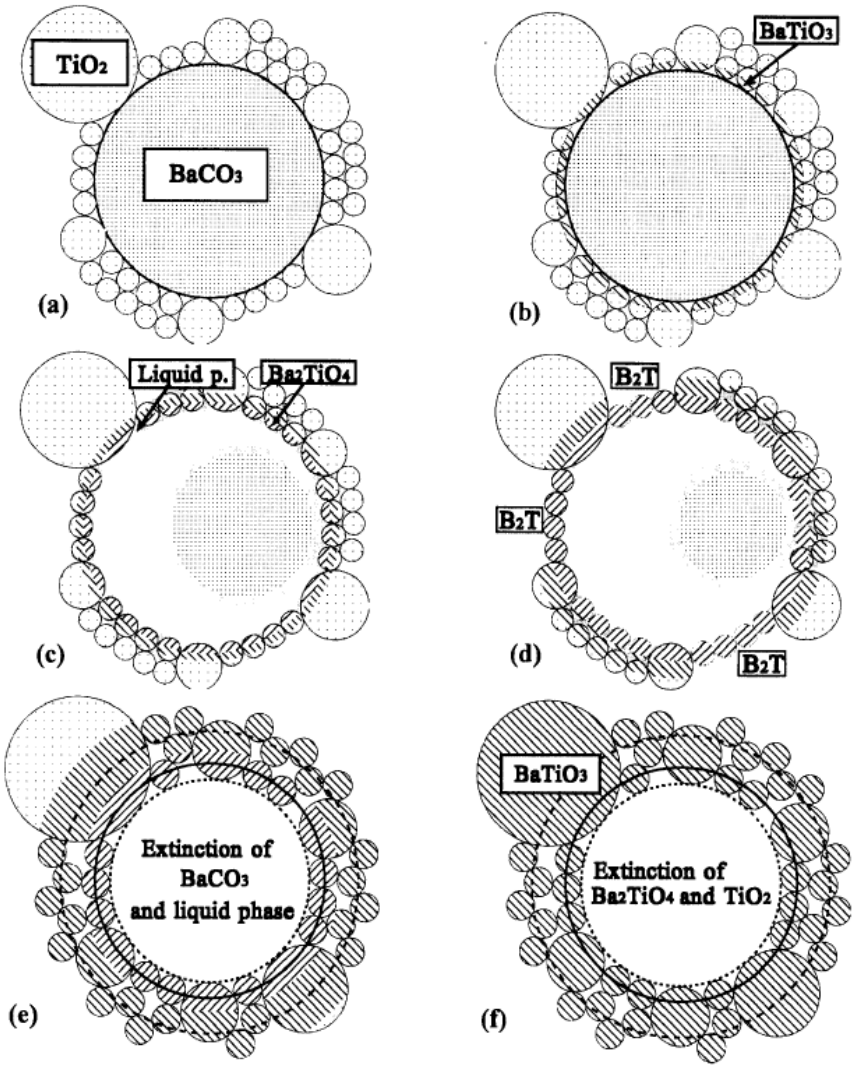

Fig. 7. Schematic evolution of a $BaCO_3$ particle surrounded by TiO_2 particles during preparation of $BaTiO_3$.
(a): Before reaction, (b): Formation of $BaTiO_3$, (c): appearance of liquid phase, (d): $\boxed{B_2T}$: exposing parts of Ba_2TiO_4, (e): solid state reaction, (f): remaining $BaTiO_3$ and large pores.

Figure 3.3: Schematic evolution of a barium carbonate particle in the steps of barium titanate formation. Taken from [9]

4 Experimental techniques and procedures

This chapter introduces the basics for conducting and evaluating all experiments. Calcination experiments were conducted with a rotary tube kiln (section 4.1) and the processed powder was investigated by X-Ray diffractometry (section 4.3), B.E.T. analysis (section 4.4) and an automatic powder tester station. The calcined powder was also investigated by ICP analysis (section 4.5) to find impurities. The moisture content (section 5.3) of the raw material mixture was determined before each calcination. A series of experiments was planned with statistical means (section 4.11).

4.1 Rotary tube kiln

All calcination experiments are conducted with a Nabertherm rotary tube kiln, model RSR120.

- Tube length: 2040 mm
- Heated length: 1000 mm
- Maximum temperature: 1400 °C (dependent on tube material)
- Temperature control: in 3 separate zones, measured at heat elements
- Tube diameter: 120 mm outer, 100 mm inner
- Rotary speed: 2 rpm to 45 rpm
- Spiral conveyor speed: 0 rpm to 20 rpm
- Inclination: 0° to 10°

One installable tube is a CrFeAl - alloy named Advanced Power Metal (APM) [4]. It can be used for temperatures up to 1200 °C. The second tube is a mullite ceramic tube of the material C610 (62.6 % Al_2O_3, 37 % SiO_2) [2].

The kiln offers continuous addition of material via a screw conveyor and a tapping mechanism for the metal tube. Gas proof conditions, a controlled atmosphere or an open process are possible. A photograph of the set-up can be found in Figure 4.1.

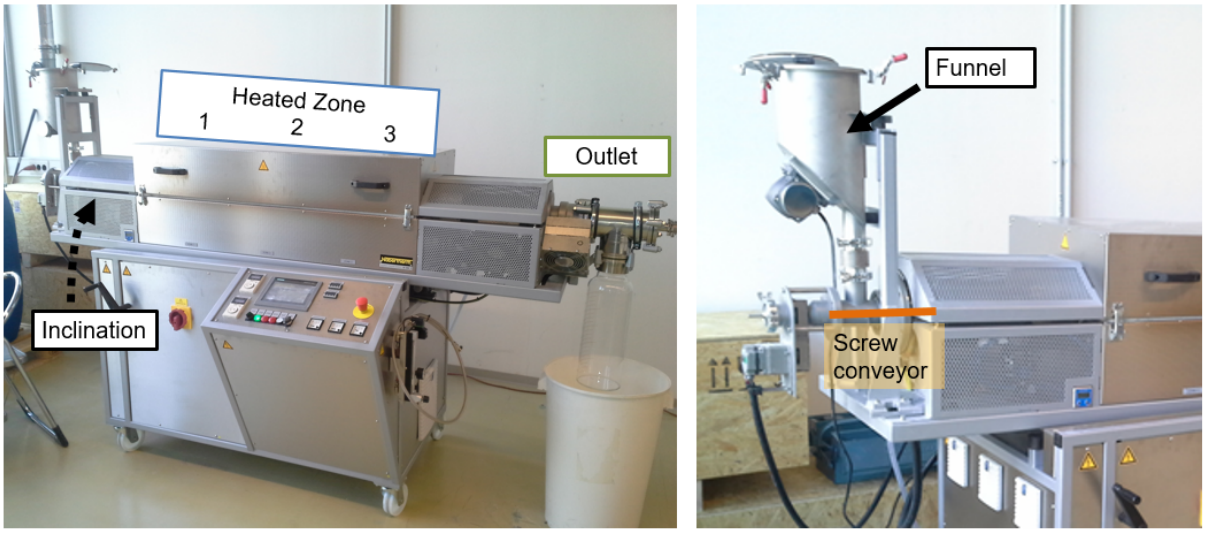

Figure 4.1: Rotary tube kiln, model Nabertherm RSR120. Material flow from left to right. Heating in three separate zones.

The following five parameters can be adjusted for experiments with the rotary tube kiln:

- Mounted tube - metal (APM) or ceramic (C610)
- Temperature (T, T_{cal}); value at heating element / outside of tube
- Inclination (Inc)
- Screw conveyor driver speed (v_f) - translation to actual rpm 1:50
- Tube driver rotary speed (v_t) - translation to actual tube rotations 1:200

Additionally the period and on-time of the tapping mechanism can be set. The tapping mechanism can only be used with the metal tube installed.

After heating up, material is filled in the screw conveyor. As shown in Figure 4.2 the material, while passing a heated zone, revolves by the rotation of the tube, which

also causes material transport. The product is collected at the end of the tube. The calcination is done in an open process, gas can exit the tube.

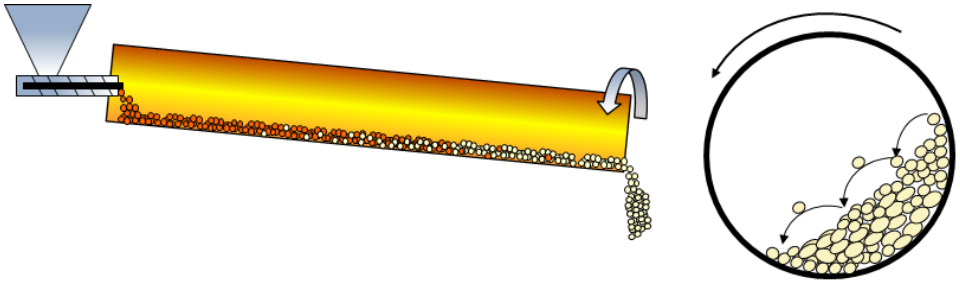

Figure 4.2: Rotary tube kiln schematic. Screw conveyor on the left side, material collection on the right end of the tube. Material flows from left to right.

It was found that after 20 min the impurities in the calcined powder sink to an acceptable level, see Figure 5.11. Therefore material of the first 20 min at least is discarded at the beginning of every experiment to avoid contamination.

4.2 Raw material

The used raw material is first mixed in a wet process, pressed trough filters and dried. Material provided for calcination consists of agglomerates of different sizes with diameters up to about 10 mm.

4.3 X-Ray diffractometry

The tetragonal lattice distortion (c/a ratio) is determined by X-Ray powder diffractometry.

The calcined powder to be investigated has to be ground in a mortar to give a fine powder for the measurement. It is mixed with a fixed amount of corundum, which serves as a standard in the measurement and allows a correction polynomial to be calculated.
A Copper source is used for the X-Ray measurements with 45 kV at 40 mA.

All measurements are done in theta-2theta scanning mode.

After the measurement the lattice parameters are determined by the Rietveld method, which is matching a mathematical function to the measured spectrum.

4.4 Specific surface area analysis - B.E.T.

The specific surface area (SSA) gives a surface area per mass and is determined by the B.E.T. method first introduced by Stephen Brunauer, P. H. Emmett and Edward Teller. [11]

For this analysis the calcined powder is sieved with a structure size of 500 µm. A weighted amount of powder is placed in a chamber and nitrogen is lead in. The sample is cooled with liquid nitrogen and some nitrogen is adsorbed which results in a change of pressure. The surface area per volume can be calculated based on this measurement. If the powder density is known a specific surface area can be determined ($m^2\,g^{-1}$). Before measurement the sample has to be heated to free adsorbed water.

4.5 Inductively coupled plasma atomic emission spectroscopy

In ICP analysis a plasma is generated by an intense electromagnetic radio frequency field in a so called torch. The typical gas used for plasma creation is Argon and can reach very high temperatures of about 6000 K.
The sample is prepared in aqueous or organic solution and sprayed as very fine drops into to the plasma. It is excited in the plasma and emits radiation of characteristic wavelengths. This radiation is detected and the information can be used to determine the elements involved. When all elements are determined standards of known concentration can be produced and used to calculate the concentration of elements in the original sample.

4.6 Moisture content analysis

The moisture content in the powder is determined by permanent weighing of the powder in a heating apparatus. Only raw material mixtures are measured (before calcination). About 20 g of powder is held at 110 °C for 15 min. A percentage of moisture in the powder sample can be calculated from the lost weight.

4.7 Powder and green body properties

A powder tester station is used to determine various properties automatically within the apparatus. The investigated material is a milled and spray-dried calcined powder, which contains a binder material.

Powder properties are as follows: [8]

- Apparent density (Schüttdichte) in $g\,cm^{-3}$ - is the weight of an unit volume of loose powder
- Tapped density (Stampfdichte) in $g\,cm^{-3}$ - powder density when the container is tapped or vibrated at specified conditions, established by ISO 3953
- Angle of repose (Böschungswinkel) in degree - calculation of the tangent of the angle as the ratio of the height to the mean base radius of a powder heap
- Maximum pressing power (Pressdruck) in MPa - pressure needed to achieve a given density (e.g. $3.42\,g\,cm^{-3}$) of the green body.
- Radial resilience (radiale Auffederung) in percent - radial change of size after release from shaping model (press form), measured with micrometer screw gauge
- Axial resilience (axiale Auffederung) in percent - axial change of size after release from shaping (press form), measured with micrometer screw gauge
- Axial green strength (Grünfestigkeit) in MPa - strength which can be applied until the green body breaks apart, a green body is crushed while measuring the applied pressure
- Radial green strength (Grünfestigkeit) in MPa - strength which can be applied until the green body breaks apart

- Cohesion - the ratio of axial green strength to the pressure applied for ejecting the green body. The green body might break apart at ejection for values greater than 1.

4.8 PTC preparation

After calcination the material is milled to a given grain size which varies with material composition. The milled material is spray-dried after adding a binder. The powder is pressed in disk-like shapes to a density of $3.42\,\mathrm{g\,cm^{-3}} \pm 0.7\,\%$.
The first sintering is done for all parts with a standard temperature profile, which is shown in Figure 4.3.

After this first sintering the room temperature resistance (R_{25}) is measured and should be between $9\,\Omega$ and $11\,\Omega$.

All parts that do not fall into this range of resistance are sintered again with a new profile until a R_{25} value in this range is realized.

Only afterwards the resistance temperature characteristics is measured.

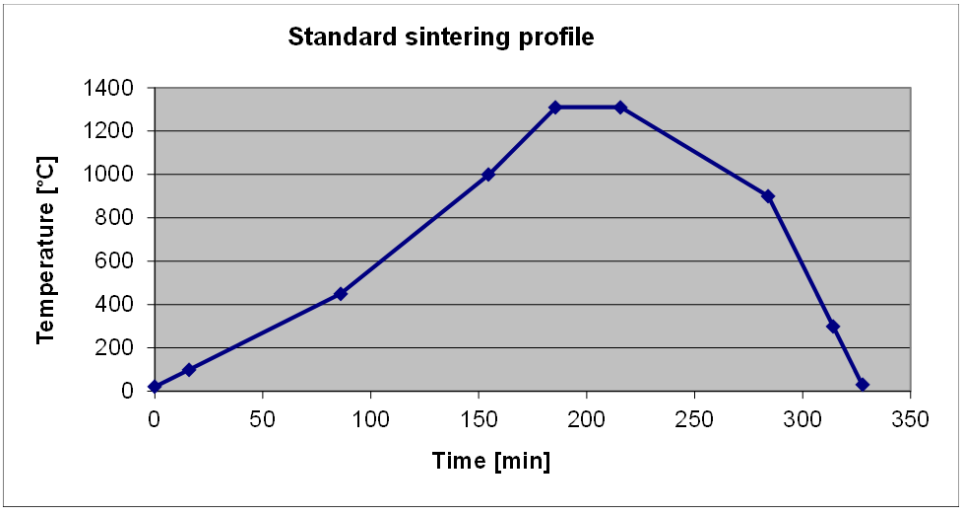

Figure 4.3: Sintering profile used for sintering EB271 PTC parts.

4.9 Room temperature resistance measurement

The resistance at room temperature (R_{25}) is measured directly after the first sintering step (see above, section 4.8). A very soft metal alloy is used to metallize the parts and the resistance is measured with an Ohmmeter. The value R_{25} is used throughout this work and should not be mistaken for R25* as described below.

4.10 Resistance temperature characteristics

After the final sintering step (not necessarily the first, see section 4.8, above) the electrical resistance (R) is measured at different temperatures (T).

The R-T measurement is conducted for five resistors at once in an oil bath with regulated temperature in 5 K steps. The mean value of this five resistances is used for further evaluation.

Important values representing this characteristics are R25*, T_{min} and T_{ref} (see subsection 2.2.1). Note however: R25* is not necessarily equal to R_{25}, which is measured after the first sintering step.

4.11 Design of experiments

Statistical experiment design aims to investigate a great number of parameters with reduced experimental effort. As experiments can be cost intensive, highly time consuming or limited in other ways it is often preferable to minimize the number of experiments for finding certain features. The statistical design is a very common tool in industry to achieve good process control and to study the influence of various parameters. The idea is to take all measurements into account when calculating the influence of a single parameter. This is in contrast to changing a single parameter and observing the influence in following measurements. More details for methods and

statistics can be found in [5, 10]. Companies often also apply the ideas of a Six-Sigma strategy. More information about this can be found in relevant books [12, 6].

A short example describes two facilities (set-ups) that are investigated as well as the influence of temperature. Like all experiments and measurements aim to achieve a certain accuracy, in this example the desired accuracy requires eight experiments for investigation of a parameter. It is often suggested to change one factor (here: facility or temperature) at a time, so resulting changes can be referred easily. On the other hand the attempt of a design of experiments (*DoEx*) is to investigate all possible combinations of factors. This can be seen in Figure 4.4. It shows 8 measurements for facility 1, 8 for facility 2 at 30 °C and 8 for facility 1 at 50 °C when using one-factor-at-a-time (*ofaad*) method. With a *DoEx* still 8 measurements are conducted for facility 2 (4 at 30 °C and 4 at 50 °C). This means that with an overall number of 16 experiments *DoEx* provides at least as good knowledge as *ofaat* with 24 experiments for the desired accuracy. The *DoEx* provides even more knowledge, because the interactions of parameters can be calculated from the data where *ofaat* does not aim to do this.

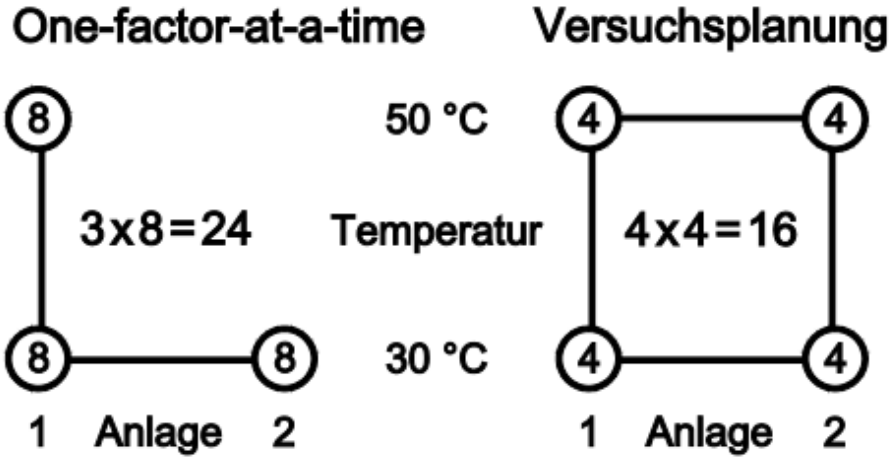

Figure 4.4: Comparison of one-factor-at-a-time to statistical plan. Two facilities and two temperatures are investigated. The number of experiments is noted. [5]

A plan of experiments can be seen as a system of equations. Each experiment corresponds to an equation.

In another example a set up with four parameters with two settings each can be fully investigated by 16 experiments (so called *full factored* plan). Interactions up to

fourth order can be found. If terms of higher order can be assumed irrelevant a partly factored plan can be constructed. A half factored plan for the example above could find interactions up to third order with only half the number of experiments (by using a subset of the equation system). This can be very useful for systems with more parameters.

A partly factored plan can reduce variance of the experiment, because more parameters are changed from one experiment to the other and the final calculations use average values. The parameters are also changed from different starting positions, which can be an advantage.

A null hypothesis analysis is calculated for all effects in the DoEx. In this theory the probability (p-value) that a measured effect is not significant is calculated. If this probability is greater than 5 % it has to be assumed that the investigated effect is not present or not significant. A very good description can be found in [10], page 95.

The DoEx allows the calculation of main effect and interaction diagrams for the experimental parameters. These diagrams are drawn for every measured or calculated quantity (electrical, powder, experimental properties). The main effect diagram shows the (neg./pos.) influence of the parameters on one quantity. The interaction diagram can be used to study the interaction of two parameters. A short explanation of the two diagrams is given in subsection 5.5.1.

5 Results

All measurement data can be found in a separate appendix book.

5.1 Determination of experimental parameters

The first step in setting up the rotary tube kiln process is to find parameters, which result in a comparable product to the standard process. The ideal values for the experimental parameters have been studied and are displayed in this chapter.

After finding usable (stable product) experimental settings, the influences of the parameters were investigated by a design of experiments which is presented in section 5.5.

The experimental settings used in the first step (before DoEx) are displayed in Table 5.1. See section 4.1 for more information on the rotary tube kiln.

Table 5.1: Experimental settings used with the Nabertherm rotary tube kiln. See section 4.1 for description of parameters.

Setting	Tube	Temperature			Inclination	Tube rotary speed		Feeding mechanism			Tapping mechanism	
		Zone 1	Zone 2	Zone 3		Electric driver	Tube	Electric driver	Rate		Period	On - time
Nr	Type	°C	°C	°C	°	rpm	rpm	rpm	kg / h		s	ms
1	APM	1050	1050	1070	1.0	1300	6.5	400	2.5	± 0.2	1	25
2	APM	1100	1100	1120	1.0	1300	6.5	400	2.5	± 0.2	1	25
3	APM	1100	1100	1120	0.5	1300	6.5	300	1.9	± 0.2	1	25
4	APM	1150	1150	1170	0.5	1300	6.5	300	1.9	± 0.2	1	25
5	APM	1150	1150	1170	1.0	1300	6.5	400	2.5	± 0.2	1	25
6	APM	1150	1150	1170	1.5	1300	6.5	500	3.1	± 0.2	1	25
7	APM	1150	1150	1170	2.0	1100	6.5	600	3.7	± 0.2	1	25
8	APM	1150	1150	1170	2.5	1100	6.5	750	4.7	± 0.2	1	25
9	C610	1100	1100	1100	1.0	1300	6.5	400	2.5	± 0.2	-	-
10	C610	1100	1100	1100	1.0	1300	6.5	600	3.7	± 0.2	-	-
11	C610	1100	1100	1100	0.5	1300	6.5	300	1.9	± 0.2	-	-

5.1.1 Motivation

The influence of calcination temperature (T_{cal}) on specific surface area (SSA) and tetragonal lattice distortion (c/a ratio) is studied.

A decrease of SSA with T_{cal} is shown in Figure 5.2. An increase of tetragonal lattice distortion can be observed with rising T_{cal} and is shown in Figure 5.3. The change of phase composition with T_{cal}, which can be used to estimate the completion of calcination, can be found in Figure 5.1. The orthotitanate phase vanishes for T greater than 1150 °C.

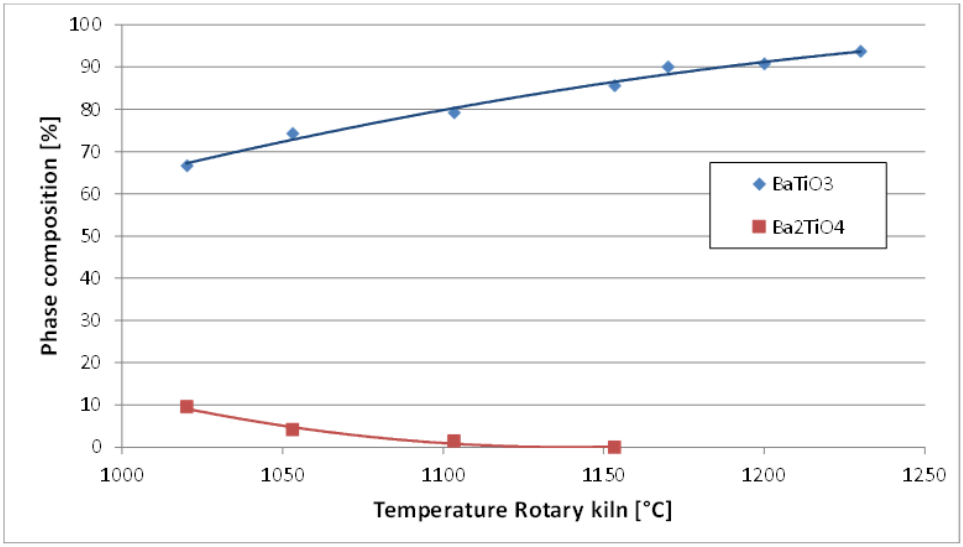

Figure 5.1: Percentage of Barium titanate and orthotitanate phases in EB222 material for different calcination temperatures.

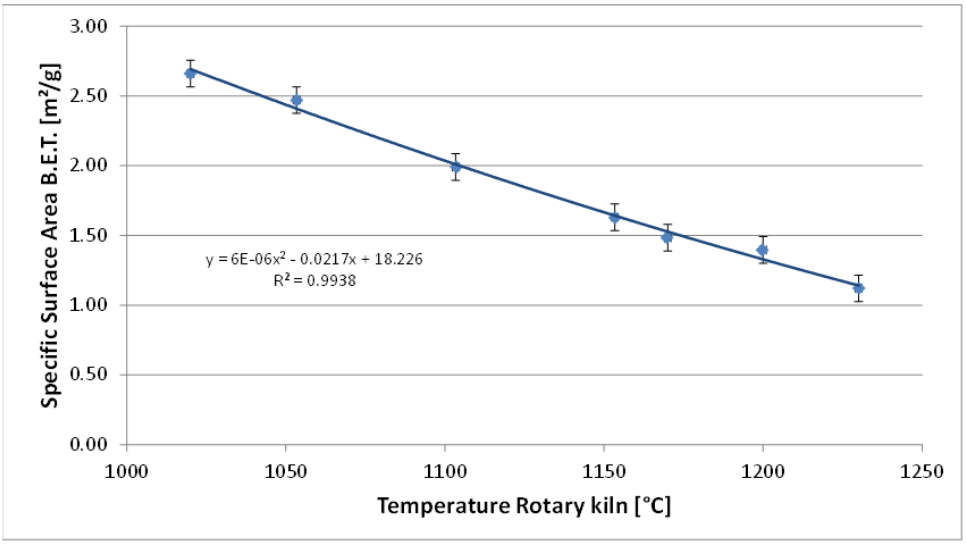

Figure 5.2: Specific surface area of EB222 material for different calcination temperatures.

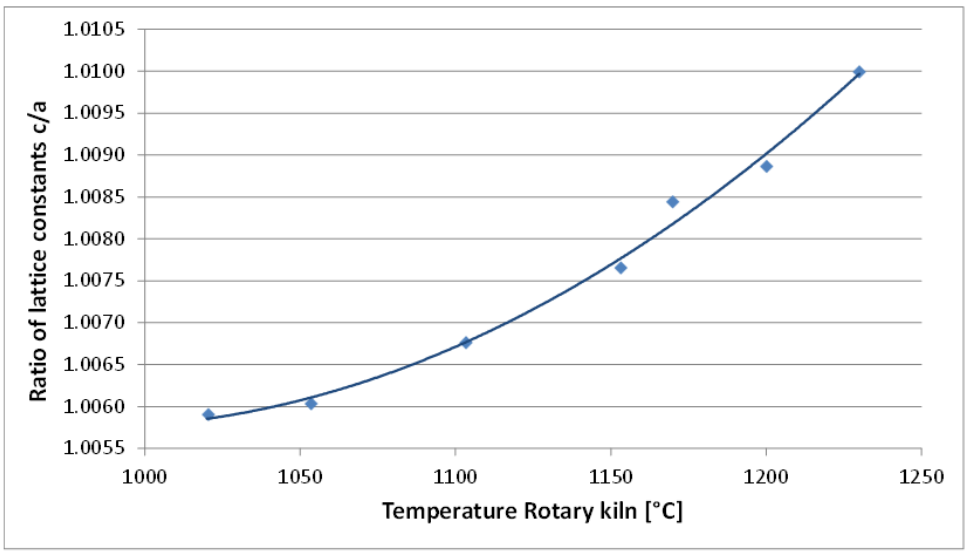

Figure 5.3: Tetragonal lattice distortion of EB222 material for different calcination temperatures.

5.1.2 Temperature

The calcination temperature T_{cal} for formation of barium titanate phase as described in section 3.2. needs to be about 1200 °C for lead free materials. For lead containing EB271 material, however, T_{cal} in the standard pusher kiln process is 1050 °C. Because of the shorter processing time also higher temperatures were investigated in the rotary tube kiln. T_{cal} of 1050 °C, 1100 °C and 1150 °C were tested.

The electrical measurements (R-T) of the final PTC product for these calcination temperatures are shown in Figure 5.4. A reference sample from the standard process can also be found there. A tendency to a lower resistance curve with higher temperatures can be seen and is also proven in Figure 5.31.

All three different temperatures are suitable for calcination, as the electrical properties are in an acceptable range.

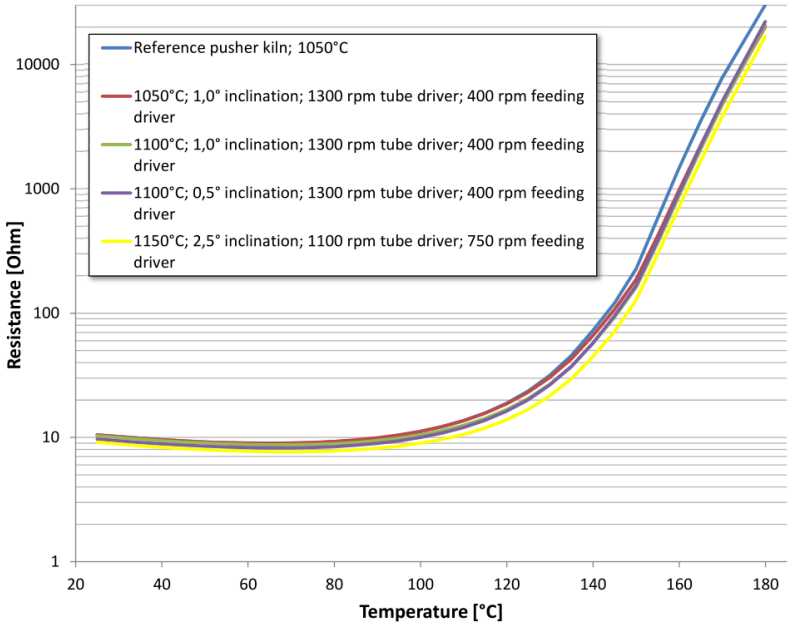

Figure 5.4: Resistance versus temperature measurements for EB271 at different process settings of the rotary tube kiln in comparison to a reference sample from pusher kiln.

5.1.3 Tube driver speed

The translation from tube rotary speed (e.g. 6.5 rpm) to driver rotary speed (e.g. 1300 rpm) is 1:200. In this work the driver speed is given in figures and tables rather than the actual tube rotary speed as it is the value that can be set on the control panel of the kiln.

The rotary speed of the tube can be assumed to influence the amount of material in the tube (filling grade) as well as the time in the heated zone.

Speeds of 1100 rpm and 1300 rpm were tested (see also Table 5.1). Further investigation of tube speed is done in section 5.5.

5.1.4 Feeding rate

The translation from spiral conveyor speed (e.g. 8 rpm) to its driver rotary speed (e.g. 400 rpm) is 1:50. Values given in figures and tables refer to the driver speed.

The feeding rate can influence the filling grade and the in- and output of material in combination with other parameters.

Material input in kg per time was measured for 3 different driver speed settings (from Table 5.2 and two additional experiments) and is shown in Figure 5.5. A linear variation of the feeding rate with the driver speed can be discerned.

5.1.5 Tube inclination

The inclination of the tube was varied from an angle of 0.5° to 2.5°. It influences the dwell time of material in the heated zone as well as the filling grade of the tube. Figure 5.6 shows that only a slight effect of tube inclination on electrical properties (final PTC product) can be observed. The tube driver speed and feeding rate were adjusted to ensure a filling grade of 5 % minimum for this experiments.

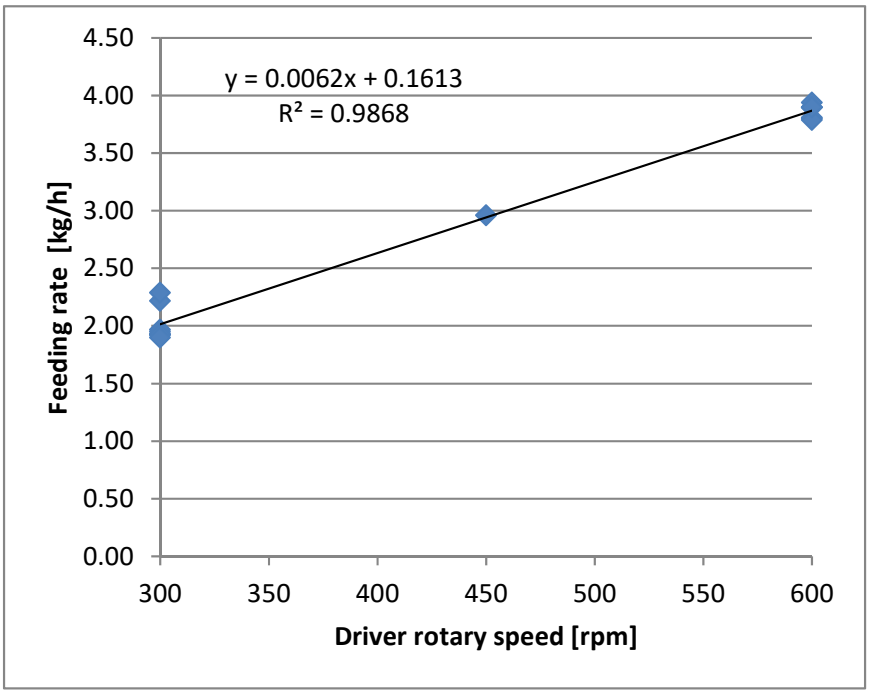

Figure 5.5: Variation of feeding rate with driver rotary speed. Number of measurement points: 300 rpm and 600 rpm 8 experiments each, 450 rpm 2 experiments

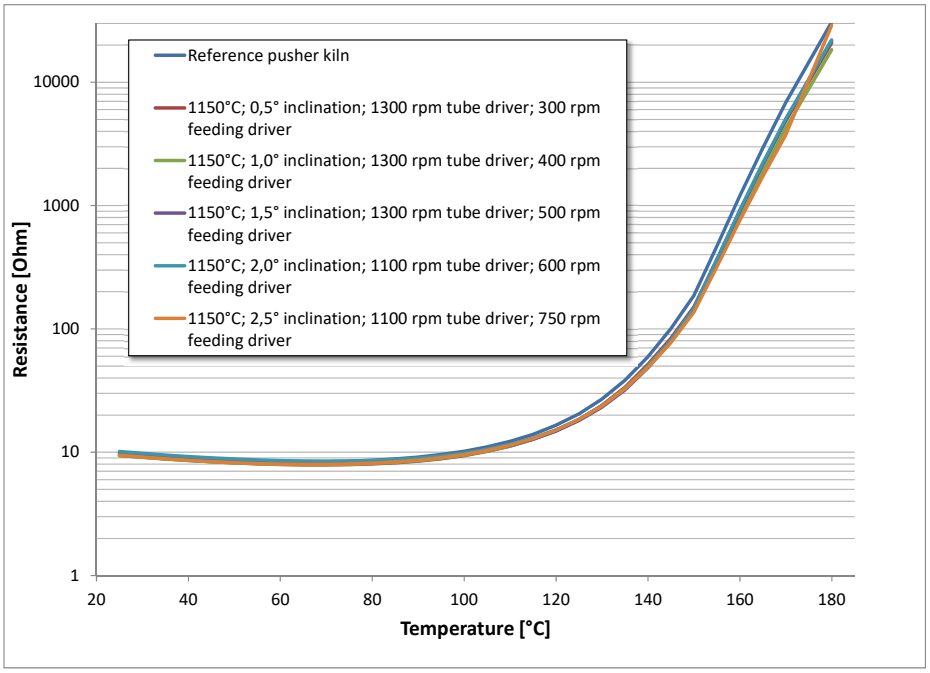

Figure 5.6: Resistance versus temperature measurements for PTCs calcined at tube inclination angles from 0° to 2.5°.

5.2 Reproducibility of experimental results

The setting 2 from Table 5.1, i.e.

- Temperature: 1100 °C
- Inclination: 1.0°
- Tube driver speed: 1300 rpm
- Feeding driver speed: 400 rpm

offers a good match of electrical properties with the reference sample of the pusher kiln for EB271. To investigate the reproducibility of the process, these settings have been used with different batches of the same raw material mixture. The experiment has been conducted non-consecutively on different dates. This is shown in Figure 5.7.

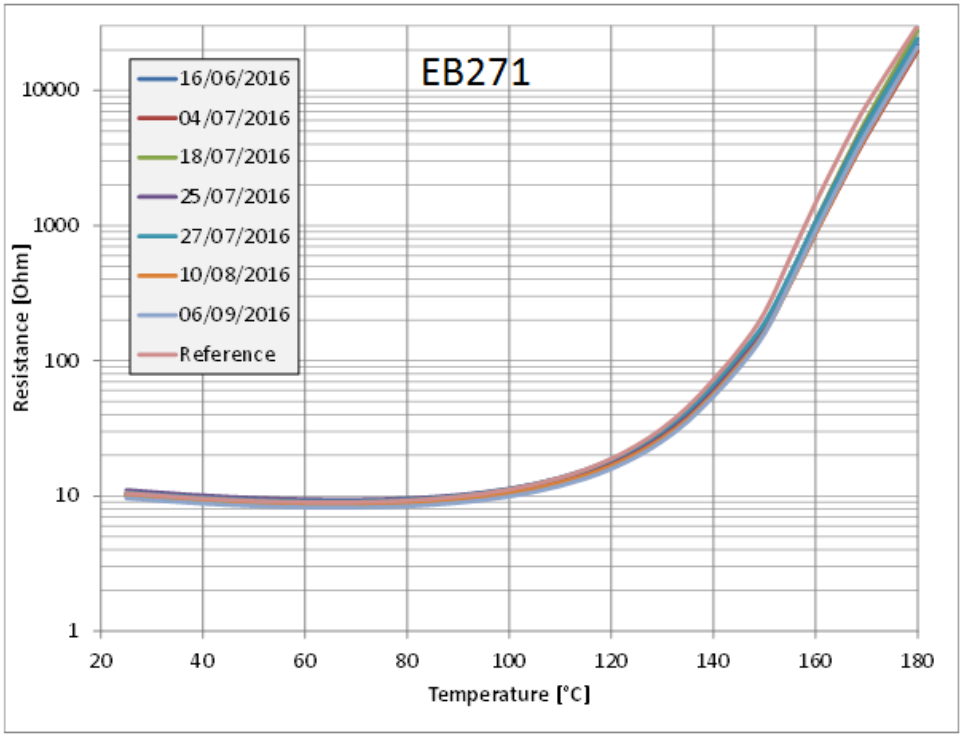

Figure 5.7: Temperature dependence of resistance. Measurements for different batches of EB271 raw material mixture. Experiments conducted non-consecutively on given dates.

Two settings of 1.7° inclination, tube driver speed of 1300 rpm and feeding driver speed of 400 rpm at temperatures 1100 °C and 1150 °C were tested for calcination of lead-free EB311. Figure 5.8 shows a rather high deviation from the reference sample.

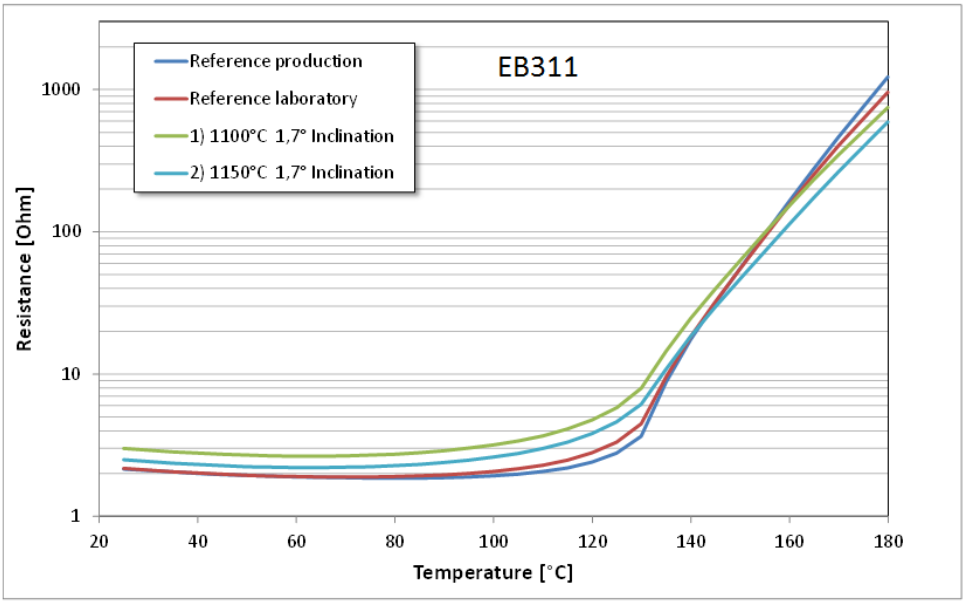

Figure 5.8: Temperature dependence of resistance for experiments with EB311.

5.2.1 Long term experiments

A long term experiment over five days time has been conducted to test the process stability in production scale amounts. One batch of 250 kg material has been processed and samples were taken every 10 h. The experimental parameters are setting 2 from Table 5.1.

The temperature dependence of resistance for the samples taken every 10 h can be found in Figure 5.9. A very low deviation can be deduced for longer time periods.

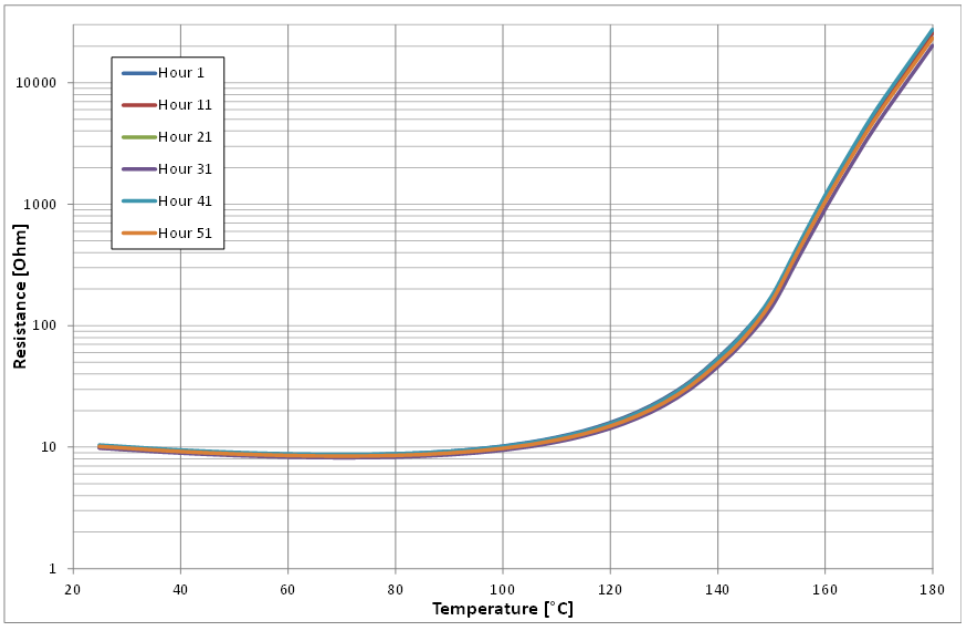

Figure 5.9: EB271 Resistance versus temperature for different sample time after experiment start of the long term experiment on 28.11.2016 11:35.

5.2.2 Time stability of SSA and c/a ratio

Used setting is number 2 from Table 5.1.
The process stability was studied from the following two points of view:

- Within **one** experiment: samples taken every few minutes
- **Different** experiments: samples taken at rerun of whole experiment

The stability measurements of tetragonal lattice distortion can be found in Figure 5.10a. The uncertainty of a single measurement (0.00012, determined by Rietveld method) is also displayed. The standard deviation (statistics for all experiments with same settings: 1.01014 ± 0.00045) for repetition of an experiment is higher than the single measurement uncertainty. Therefore this higher value has to be taken into account when interpreting dependencies.

The stability of the specific surface area (SSA) is shown in Figure 5.10b. The uncertainty of a single measurement ($0.1\,m^2\,g^{-1}$, determined by B.E.T. method) is also displayed. The standard deviation (Std-dev) of all measurements during one single experiment equals this uncertainty. Std-dev (statistics for all experiments with same settings:

$1.60\,\mathrm{m^2\,g^{-1}} \pm 0.03\,\mathrm{m^2\,g^{-1}}$) for repetition of an experiment is lower than the single measurement uncertainty. Therefore a very stable process can be expected.

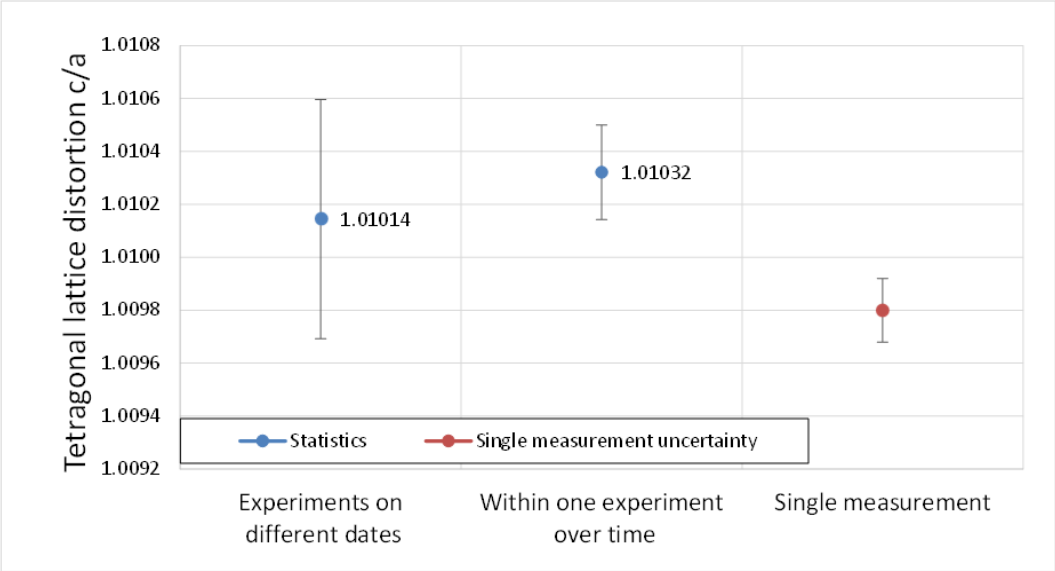

(a) Tetragonal lattice distortion (c/a ratio)

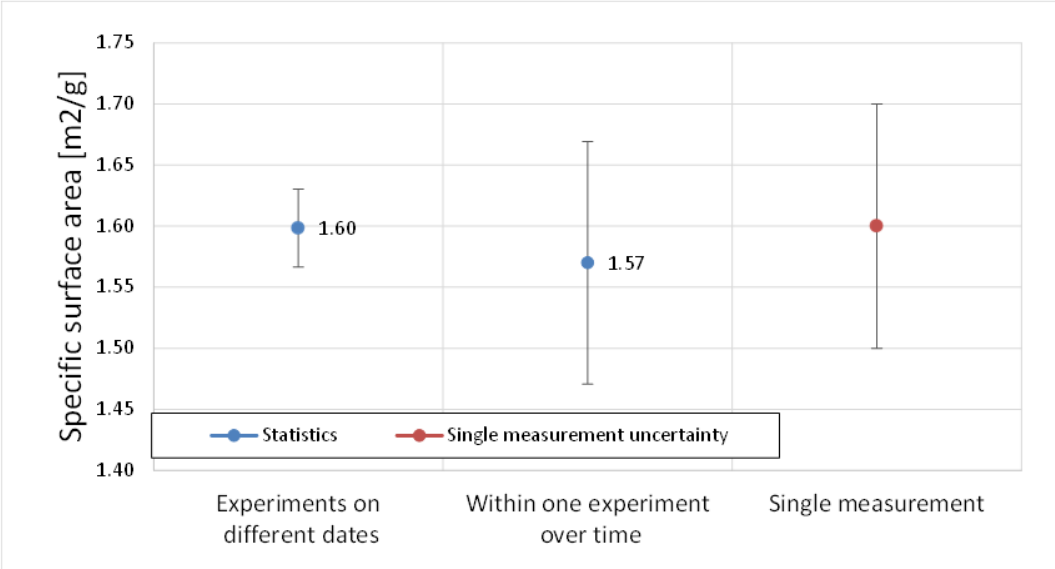

(b) Specific surface area (SSA)

Figure 5.10: Single measurement uncertainty (red), Mean value and std-dev for samples taken from rerun of experiment on different dates (left) and within one single experiment over 100 min time (right).

5.3 Moisture content analysis

It was found that raw material with a moisture content of 1.79 % wt. resulted in a high degree of humidity inside the tube during calcination. Using setting 3 (Table 5.1) for calcination resulted in a factor 3.17 higher R_{25} value than expected. This indicates an incomplete calcination.

During the experiment condensing water was observed at the outlet of the tube. The process was run with standard opening (about 5 mm diameter) at feeding side of tube opened.

5.4 Analysis of impurities

The amount of impurities in the calcined powder (APM tube, setting 2 from Table 5.1) was investigated by inductive coupled plasma analysis. A decrease of impurity concentration can be seen in Figure 5.11. The level of 5 ppm is reached after about 20 min and no increase is observed.

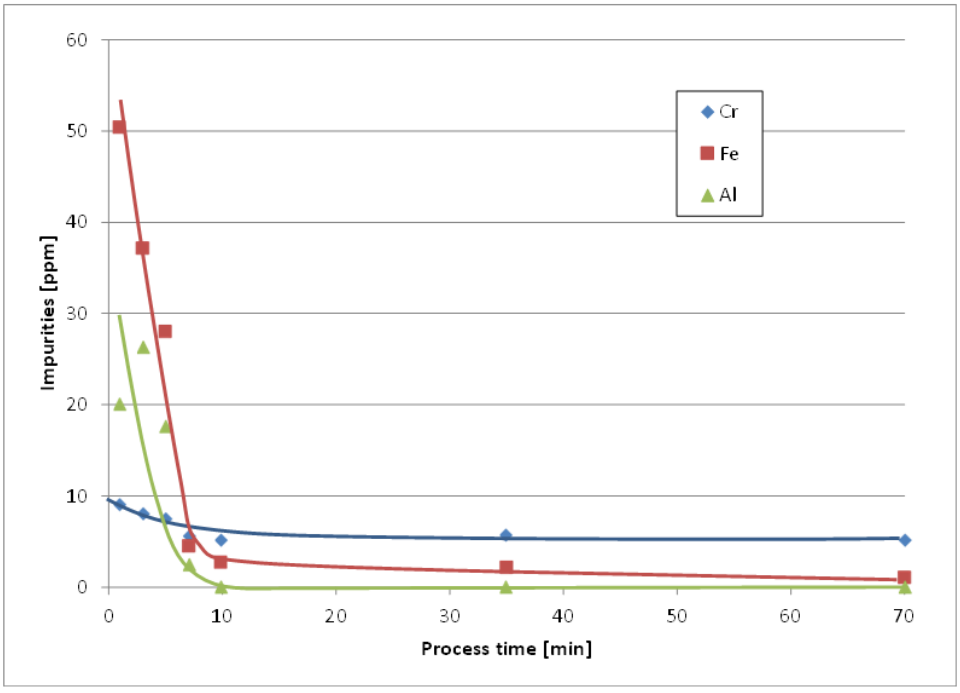

Figure 5.11: Impurities in calcined material over sample time.

5.5 Design of experiments

The influence of experimental parameters on PTC/powder features has been investigated by a design of experiments (see section 4.11).

The five parameters, for which two points have been chosen, are:

- Tube type: APM - Metal alloy, C610 - ceramic tube
- Temperature: 1050 °C and 1150 °C
- Inclination: 0.5° and 1.5°
- Tube driver speed: 1000 rpm and 1500 rpm
- Feeding driver speed: 300 rpm and 600 rpm

A half-factored series of experiments has been designed. These 2^{5-1} experimental settings and some results for this series are shown in Table 5.2.

Table 5.2: Design of experiments (DoEx) - Series of experiments with settings and results of throughput, specific surface area (SSA) and tetragonal lattice distortion (c/a). APM - metal alloy tube; C610 - ceramic tube

Date	Name	Temp.	Inclin.	Driver speed		Tube	Throughput	SSA	XRD
		Zone 2		Tube	Feeding	Type			c/a
dd.mm.	Nr	°C	°	rpm	rpm		kg/h	m² /g	
29.09.	V1	1050	0.5	1000	600	C610	2.74	1.92	1.00961
28.09.	V2	1050	1.5	1000	300	C610	1.64	1.92	1.00992
30.09.	V4	1150	0.5	1500	600	C610	3.13	1.44	1.00999
11.10.	V5	1050	0.5	1500	600	APM	3.11	1.80	1.00959
11.10.	V8	1150	0.5	1500	300	APM	1.57	1.35	1.01032
11.10.	V9	1050	1.5	1000	600	APM	3.23	1.92	1.00961
29.09.	V10	1050	0.5	1500	300	C610	1.57	1.70	1.00997
03.10.	V11	1150	0.5	1000	300	C610	1.53	1.35	1.01009
30.09.	V12	1150	1.5	1000	600	C610	3.14	1.45	1.01022
12.10.	V13	1150	1.5	1000	300	APM	1.61	1.35	1.01035
12.10.	V16	1150	1.5	1500	600	APM	3.28	1.44	1.01020
04.09.	V17	1050	1.5	1500	600	C610	3.24	2.81	1.01036
17.10.	V19	1050	0.5	1000	300	APM	1.43	1.92	1.00967
04.09.	V20	1150	1.5	1500	300	C610	1.58	1.55	1.01017
18.10.	V21	1150	0.5	1000	600	APM	2.75	1.31	1.01017
17.10.	V25	1050	1.5	1500	300	APM	1.74	2.20	1.00986

P-values higher than 10 % are not shown in plots, as these parameters have no significant influence on the quantity. (Values above 5 % are considered not significant)

5.5.1 Main effect and interaction plots

The **main effects** plot shows the change of a quantity (e.g. throughput) for every parameter (e.g. feeding rate) as mean values.
E.g. the plot for throughput q_t, Figure 5.12, row 2 column 2:
The mean value of q_t for all experiments with feeding rate/driver speed v_f of 300 rpm is 1.58 kg h^{-1}. This mean value is calculated from 8 experiments as shown in Table 5.2 (namely: V2,8,10,11,13,19,20,25). The mean value for all experiments with setting 600 rpm is 3.07 kg h^{-1}. This is also calculated from the values of the corresponding 8 experiments as shown in Table 5.2 (namely: V1,4,5,9,12,16,17,21).

The significance of the influences can be estimated by the given p-values, which are the probability for the null hypothesis (i.e. the probability that the influence is not significant). Only p-values less than 10 % are shown as parameters with values higher than 5 % are considered insignificant.

The **interaction** diagram can be used to study the interaction of two parameters.
E.g. the interaction plot for c/a ratio, Figure 5.15:
An interaction of tube material and temperature can be seen in row 1, column 1. The y-Axis (on the right end side) shows the values for c/a ratio. The red line (squares) shows the mean values of all experiments with APM tube at 1050 °C (left, 4 experiments: V5,V9,V19,V25) and 1150 °C (right, 4 experiments: V8,V13,V16,V21). The black line (dots) shows the respective mean values for experiments with C610 tube. An interaction is present, because the slopes of the red and black line are different. I.e. the temperature has a different influence on c/a ratio for APM than for C610 tube material. **No** interaction is present for feeding rate and temperature, row 2, column 4. The red (1150 °C) and black (1050 °C) lines show different values for both, 300 rpm and 600 rpm feeding rate. This, however, is the influence of temperature and not an interaction with feeding rate. No interaction is present because the slopes of red and black line are equal.

The values in interaction plots are means of 4 experiments each, therefore a rather high variance can be expected and the plots need to be interpreted with care.

5.5.2 Throughput

Figure 5.12 shows the main effects plot for material throughput (q_t). The mean value of q_t for all experiments with feeding rate (v_f) of 300 rpm is 1.58 kg h^{-1} and the mean value for all experiments with setting 600 rpm is 3.07 kg h^{-1}. A p-value of 0 % is given for v_f. This means the null-hypothesis (no effect present) has a possibility of 0 % and v_f is a very significant parameter.

The tube rotary speed (v_t, named rotary speed in plot) and tube inclination (I_t) also have p-values less than 5 % and can therefore be seen to have a significant influence on the material throughput.

The interaction plot in Figure 5.13 shows a slight interaction of I_t and v_t. This can be seen in the third row in the third column. For v_t of 1500 rpm (right value) both inclinations of 0.5 (black) and 1.5° (red) result in q_t of about 2.4 kg h^{-1} (y-Axis). For v_t of 1000 rpm (left value) a difference of (q_t) can be seen for the two inclination settings. This means an interaction of the two parameters could be present.

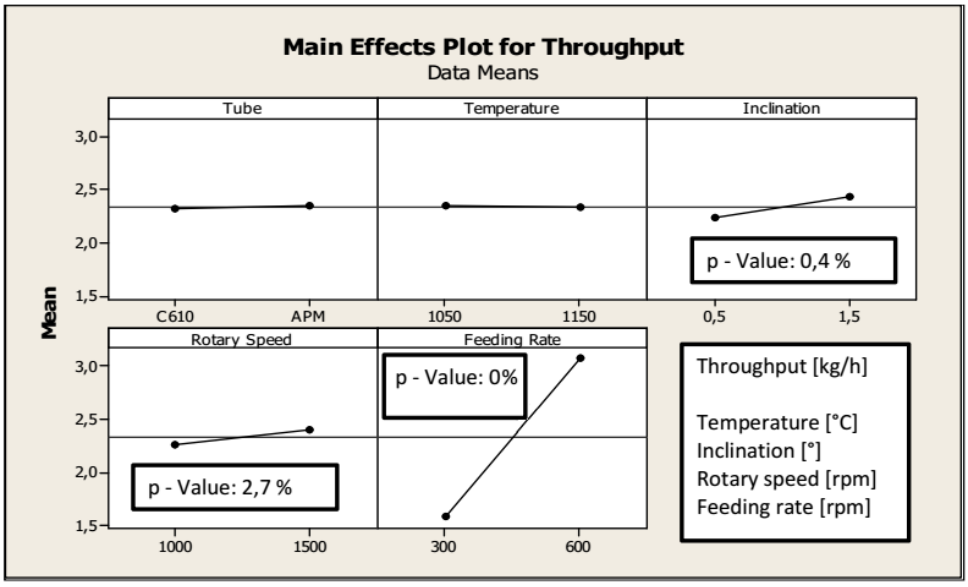

Figure 5.12: Main effects plot showing the influence of process parameters on throughput q_t.

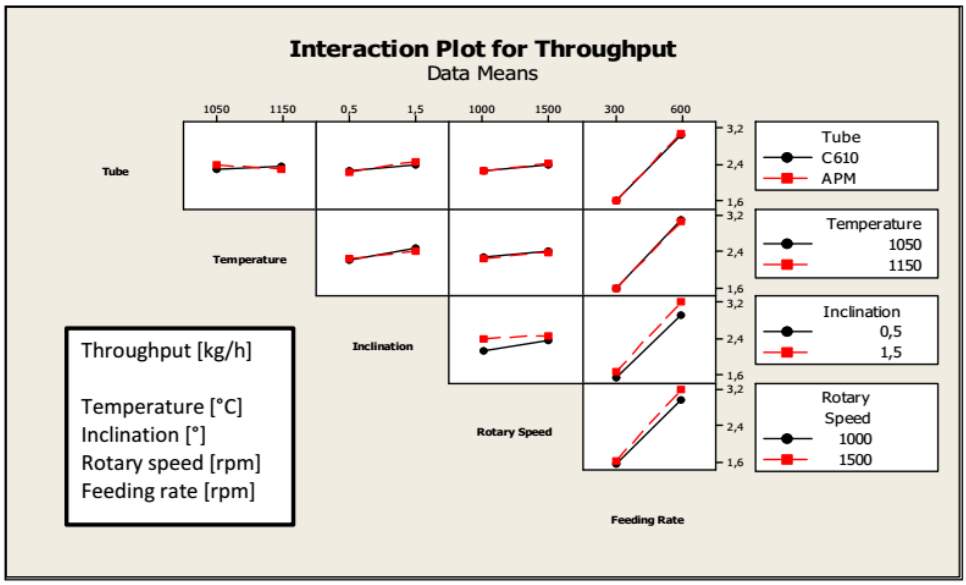

Figure 5.13: Interaction plot for material throughput showing the influence of each process parameter on the others.

5.5.3 Tetragonal lattice distortion

The main effects plot for the tetragonal lattice distortion (c/a ratio) is shown in Figure 5.14. The temperature shows a strong positive influence and is the only significant factor according to null hypothesis analysis with a p-value of 0.4 %. All other parameters show a p-value higher than 5 % and can be seen as insignificant.

The interaction plot for the ca ratio is shown in Figure 5.15. A small interaction of feeding rate (column 4) and inclination (row 3) can be seen. The feeding rate has more influence for the lower inclination (black). The calcination temperature shows higher influence for the use of APM tube (red) than for C610 tube material (column 1, row 1).

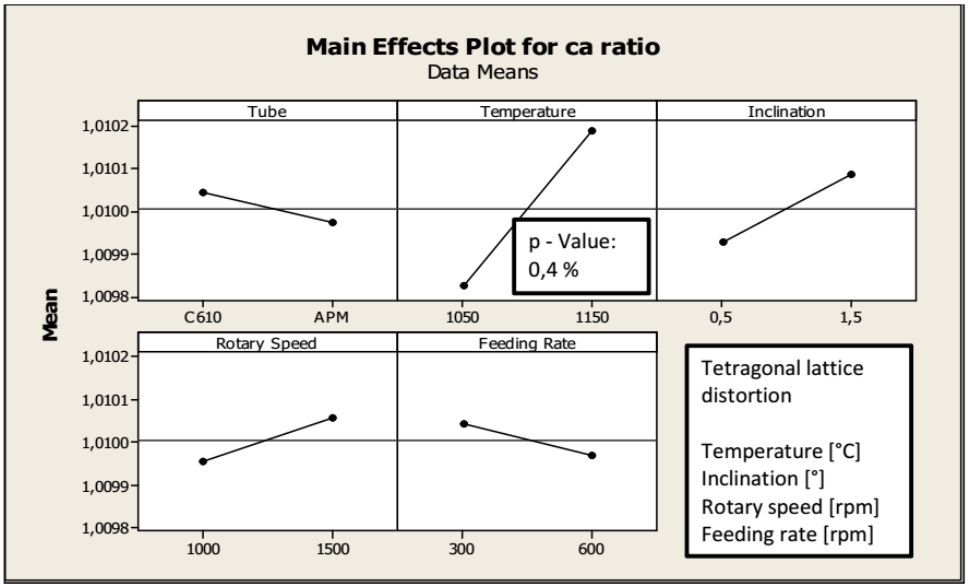

Figure 5.14: Main effects plot for the tetragonal lattice distortion (ca ratio).

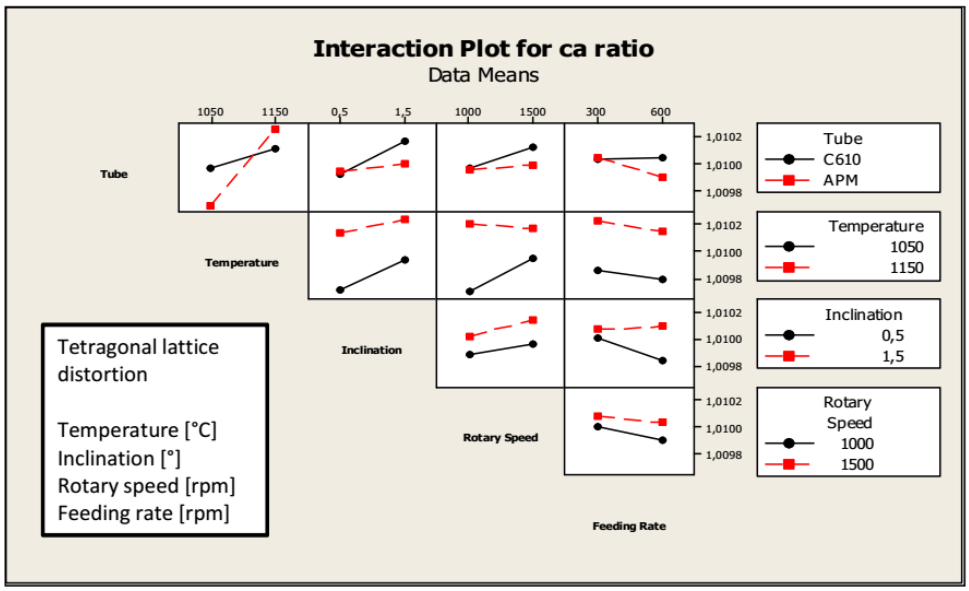

Figure 5.15: Interaction plot for the tetragonal lattice distortion (ca ratio).

5.5.4 Specific surface area

The specific surface area is measured by B.E.T. analysis.

The main effects plot for the specific surface area in $m^2\,g^{-1}$ is shown in Figure 5.16. The calcination temperature shows a strong impact and is very significant according to null-hypothesis analysis. A positive influence of the tube inclination can be seen, but is not a significant effect according to null-hypothesis analysis (p-value higher than 5 %).

The interaction plot in Figure 5.17 shows interactions of (tube) rotary speed with inclination and feeding rate with tube material.

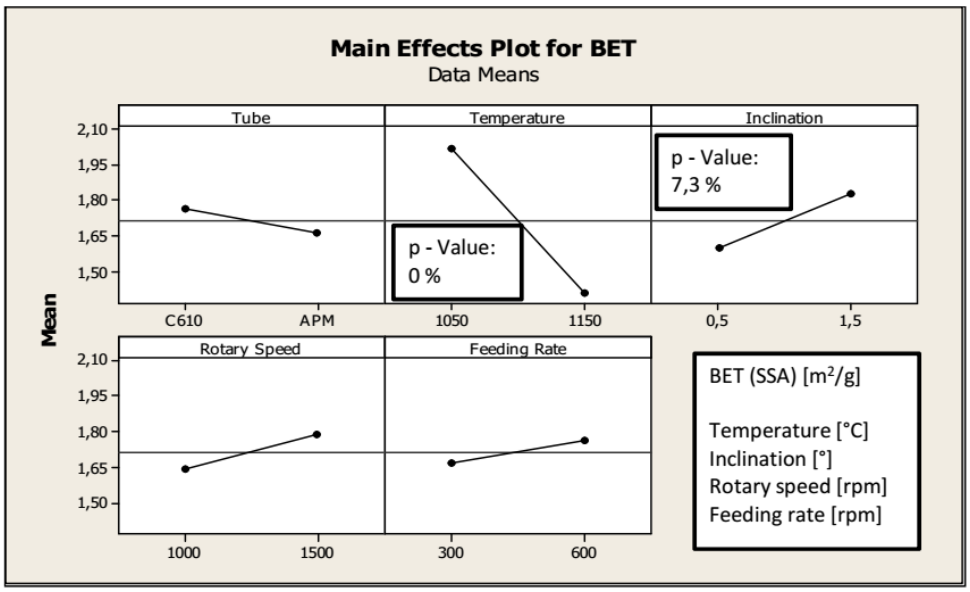

Figure 5.16: Main effects plot for the specific surface area in $m^2\,g^{-1}$.

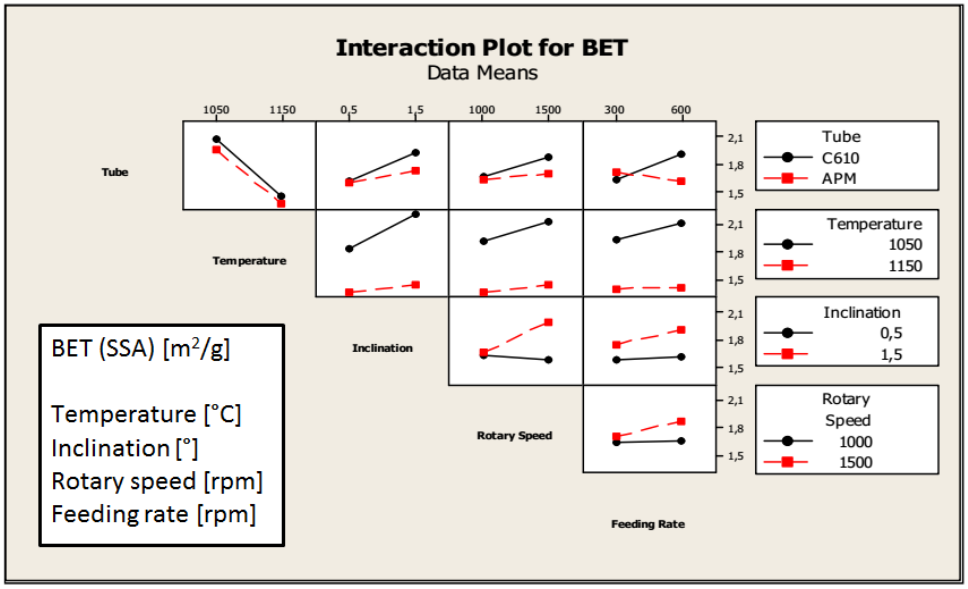

Figure 5.17: Interaction plot for the specific surface area in $m^2\,g^{-1}$.

5.5.5 Apparent density

The apparent density (Schüttdichte) main effects plot is shown in Figure 5.18. The temperature shows a rising influence and is found to be the only significant parameter (p-value of 0 %).

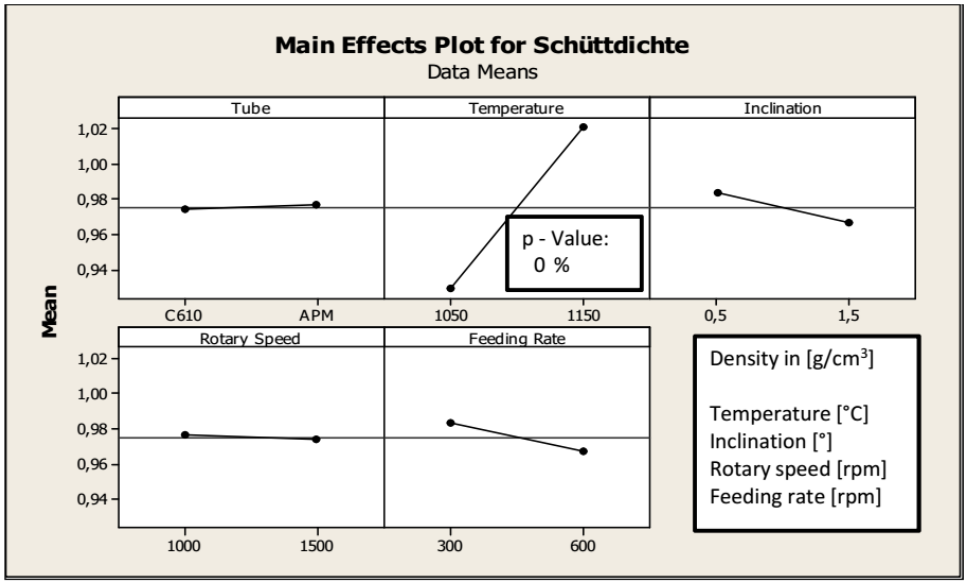

Figure 5.18: Main effects plot showing the influence of process parameters on apparent density.

The plot of the density in dependence of specific surface area (SSA) as shown in Figure 5.19 reveals a clear correlation between the two quantities, i.e. the density

decreases with increasing SSA.

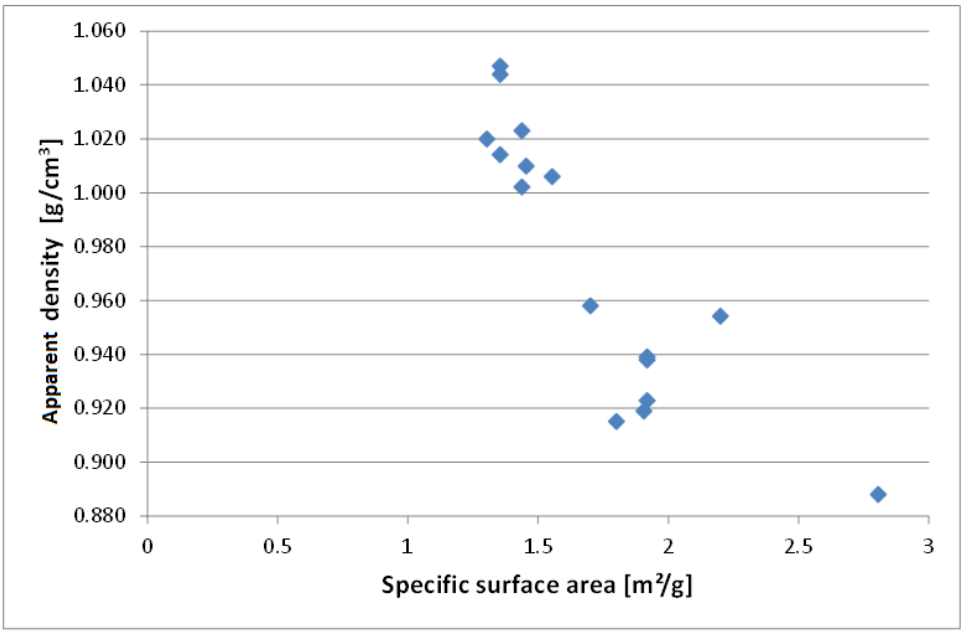

Figure 5.19: Settled density versus specific surface area.

5.5.6 Tapped density

The tapped density (Stampfdichte) main effects plot is shown in Figure 5.20. The temperature shows a rising influence and has a p-value of 0 %.

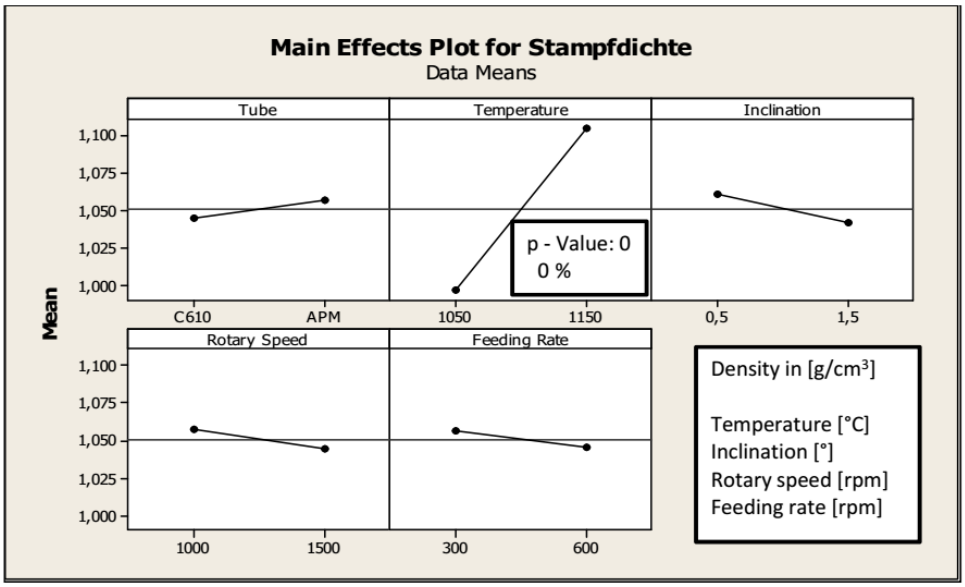

Figure 5.20: Main effects plot for tapped density.

5.5.7 Angle of repose

The angle of repose (Böschungswinkel) main effects plot is shown in Figure 5.21. The tube material has a significant influence on this value (p-value of 4 %) and shows a higher angle of repose for the APM tube.

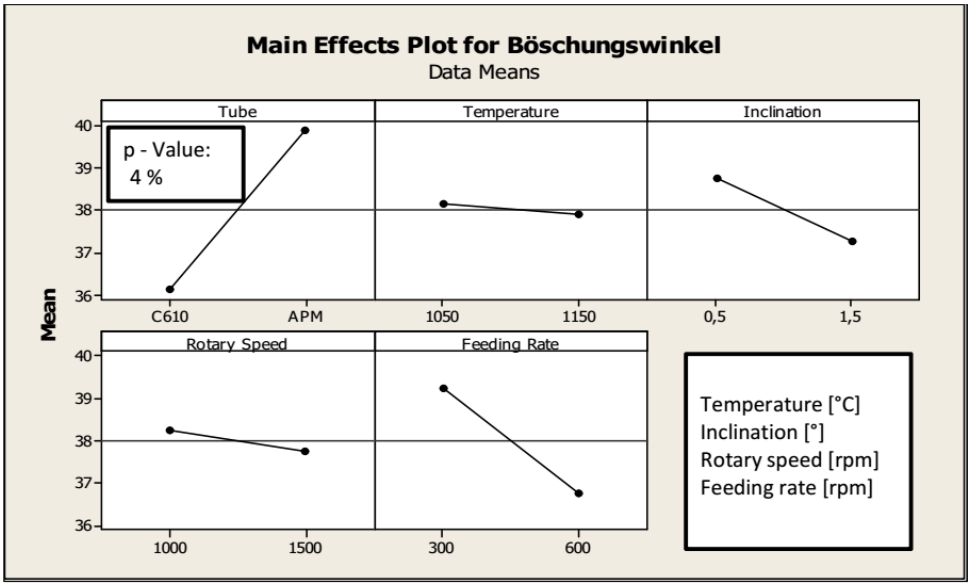

Figure 5.21: Main effects plot for angle of repose.

5.5.8 Maximum pressing power

The maximum pressing power (pressure needed to achieve a given density of the green body) main effects plot is shown in Figure 5.22. The needed pressure decreases with increasing temperature and increases with higher inclination.

A rising trend of the needed pressing power is observed with increasing specific surface area (SSA), which is shown in Figure 5.23.

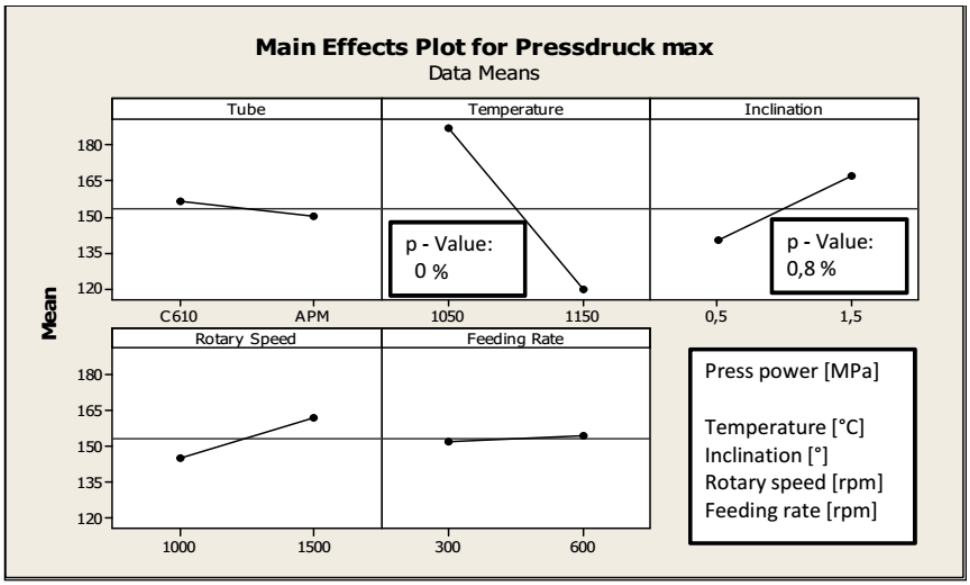

Figure 5.22: Main effects plot for maximum pressing power.

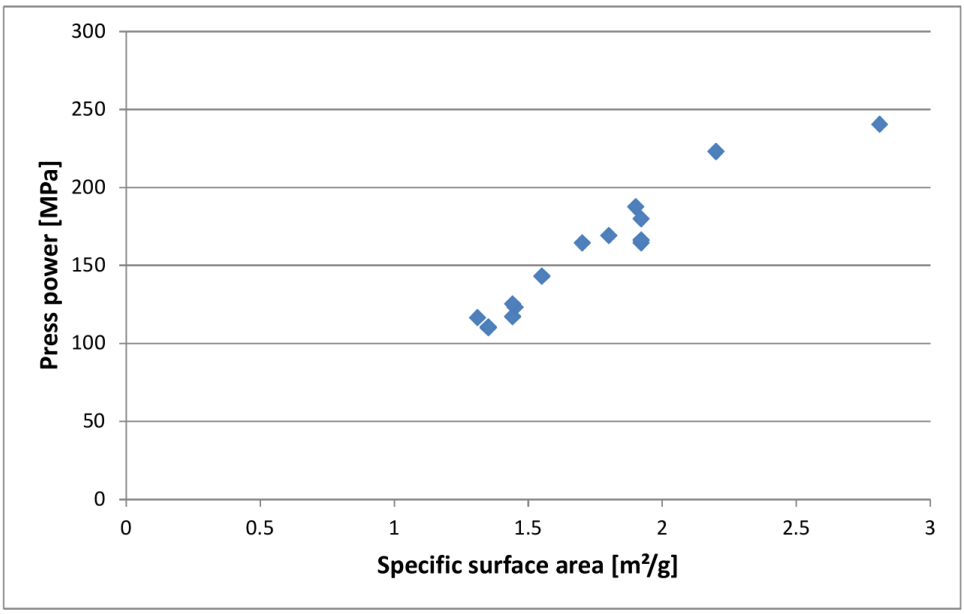

Figure 5.23: Maximum pressing power over specific surface area.

5.5.9 Resilience radial and axial

The resilience (Auffederung, change of size in %) main effects plots are shown in Figure 5.24 (radial) and Figure 5.25 (axial). A higher temperature lowers the resilience.

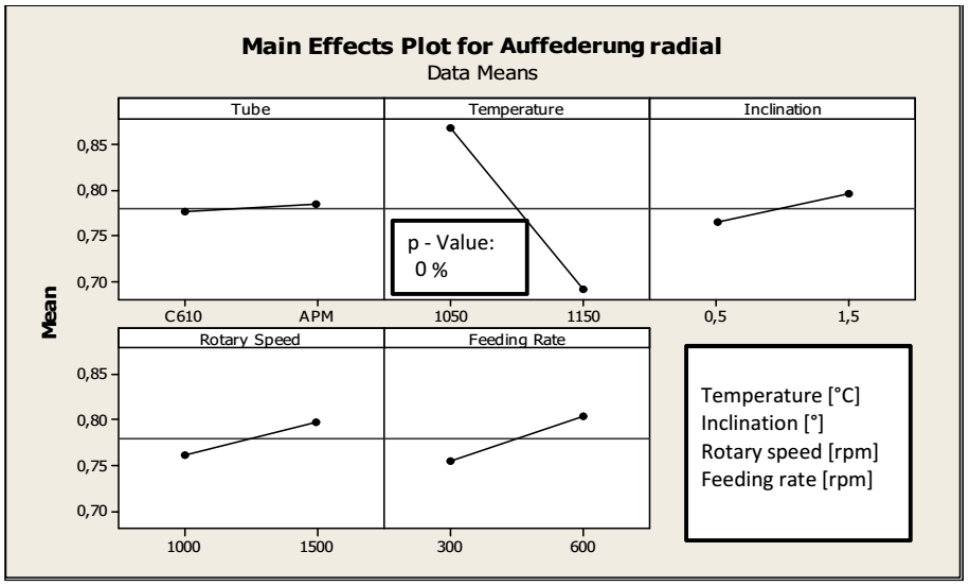

Figure 5.24: Main effects plot for radial resilience.

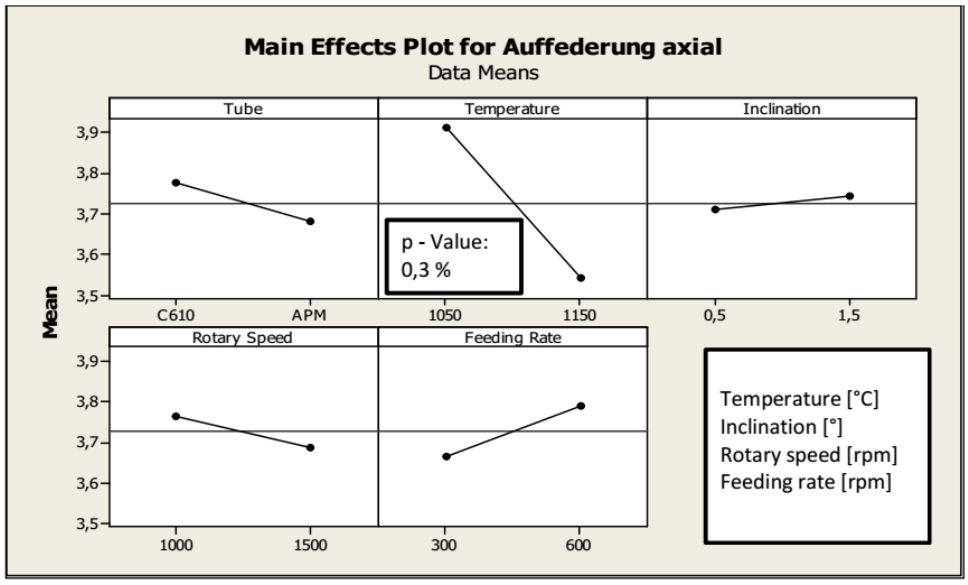

Figure 5.25: Main effects plot for axial resilience.

The radial resilience increases with specific surface area (SSA) as shown in Figure 5.26.

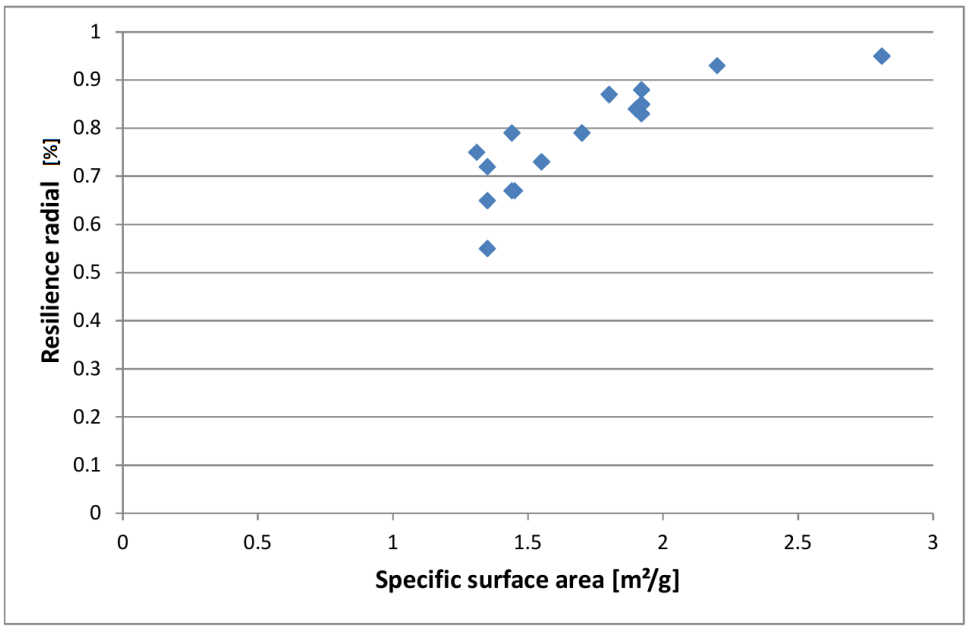

Figure 5.26: Radial resilience over specific surface area.

5.5.10 Cohesion

The cohesion main effects plot is shown in Figure 5.27. None of the parameter shows a significant influence (p-values are all higher than 5 %).

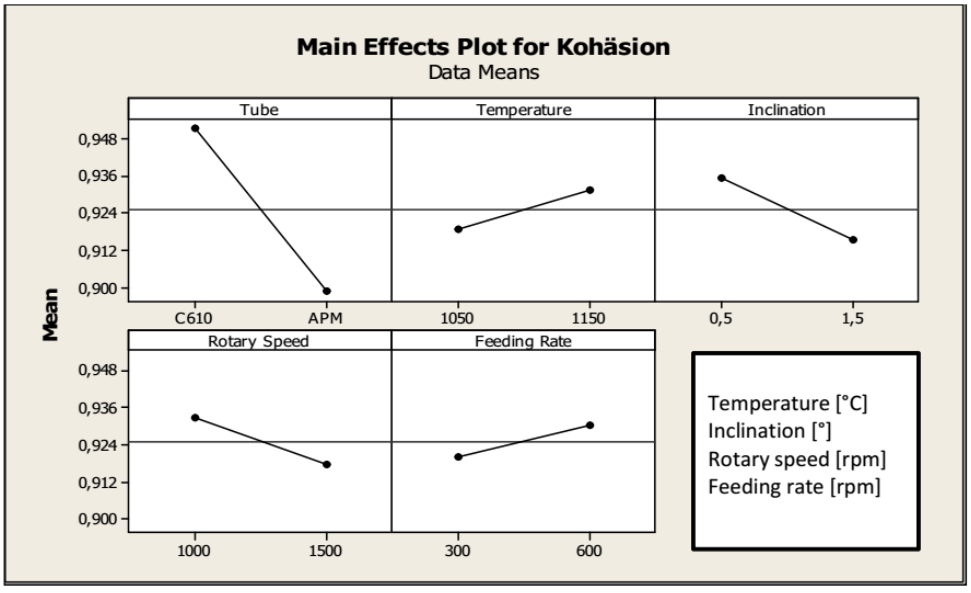

Figure 5.27: Main effects plot for cohesion.

5.5.11 Green strength radial and axial

The green strength (Grünfestigkeit) main effects plots are shown in Figure 5.28 (radial) and Figure 5.29 (axial). A higher temperature decreases these strengths.

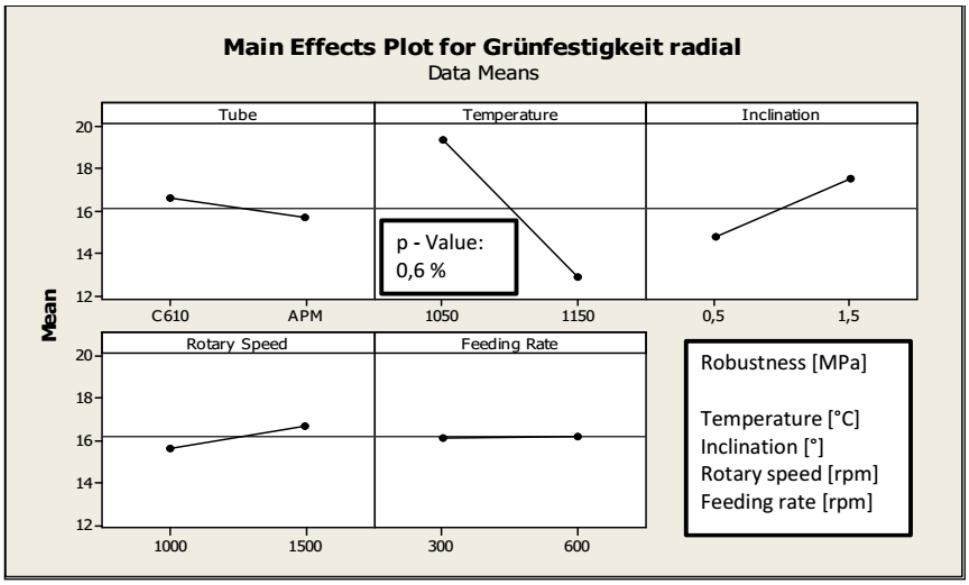

Figure 5.28: Main effects plot for radial green strength.

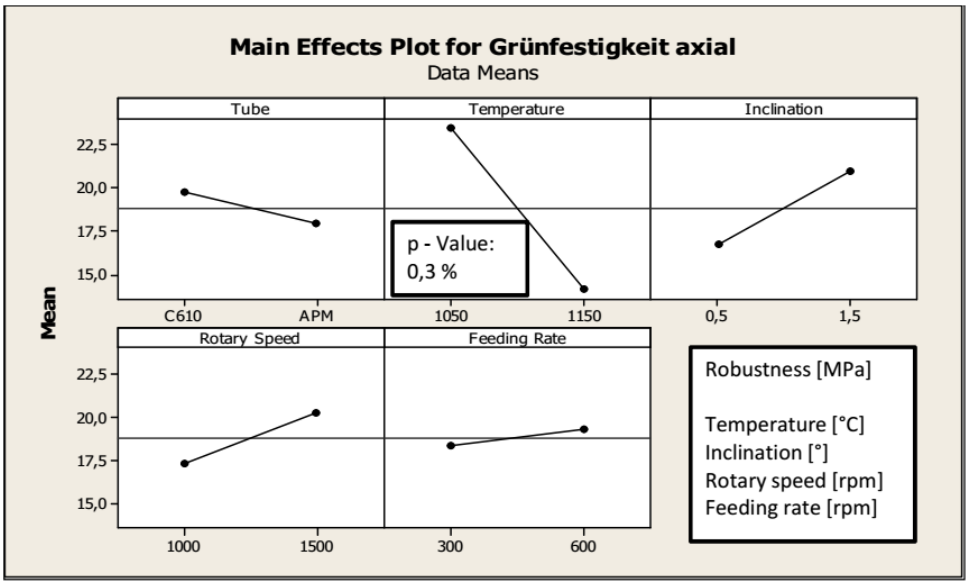

Figure 5.29: Main effects plot for axial green strength.

A positive linear dependence of green strengths on the specific surface area is shown in Figure 5.30.

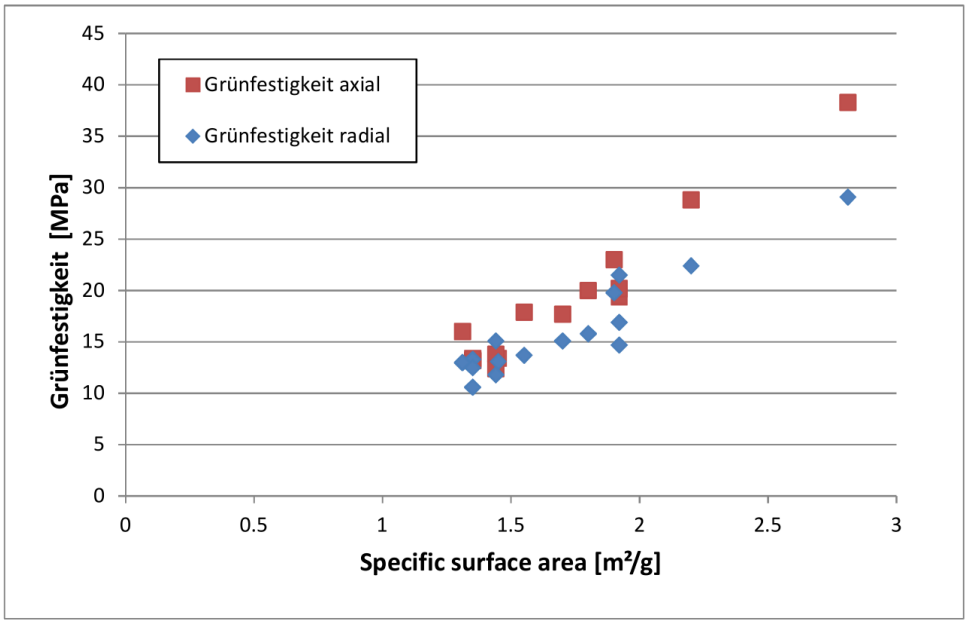

Figure 5.30: Green strength over specific surface area.

5.5.12 Room temperature resistance

The main effects diagram for the electrical resistance at room temperature (R_{25}) can be found in Figure 5.31. The only significant factor according to null hypothesis analysis (p-value of 1.1 %) is the temperature. Higher values of which lead to a lowering of R_{25}.

The plot in Figure 5.32 shows various interactions of the parameters. The inclination has more influence on the result with the ceramic (C610) tube (column 2, row 1, black line, dots). The tube driver rotary speed v_t has a positive influence on R_{25} for higher T_{cal} and a negative influence for lower T_{cal} (column 3, row 2). The feeding rate has a greater influence for lower v_t (black) than for higher (column 4, row 4).

Figure 5.33 shows R_{25} for the different values of the tetragonal lattice distortion. No dependence or correlation can be discerned.
R_{25} slightly increases with SSA, which is shown in Figure 5.34.

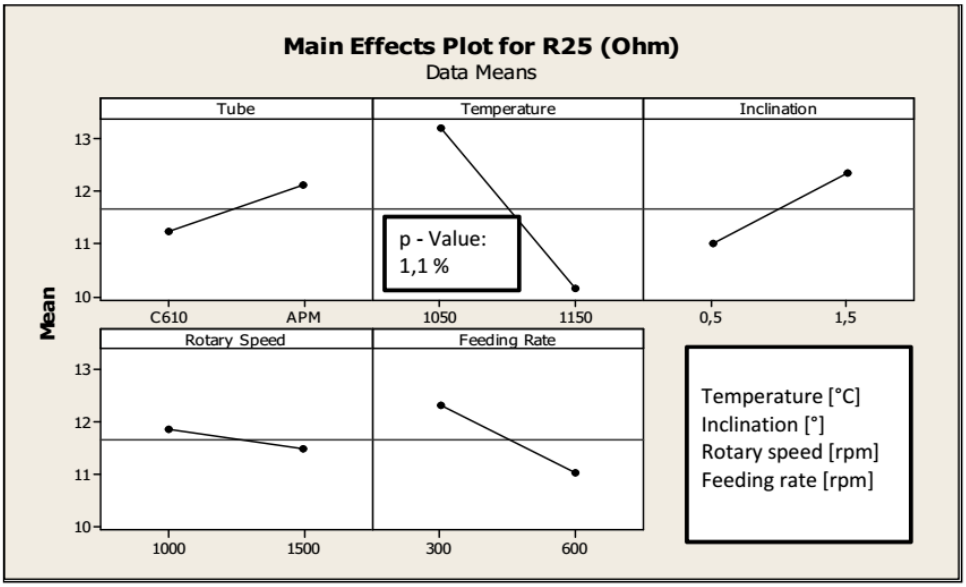

Figure 5.31: Main effects plot for electrical resistance at room temperature (R25) in Ω.

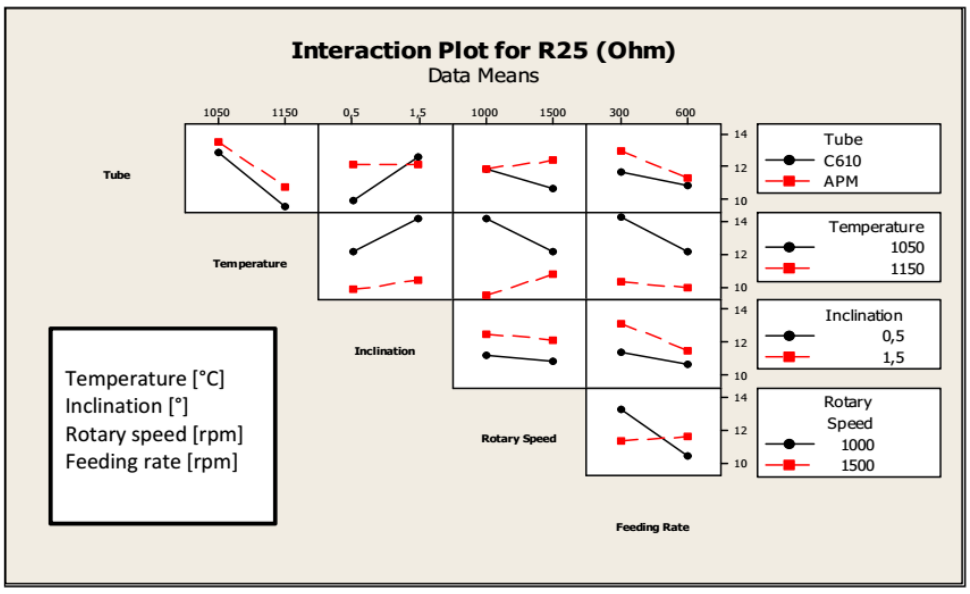

Figure 5.32: Interaction plot for electrical resistance at room temperature (R25) in Ω.

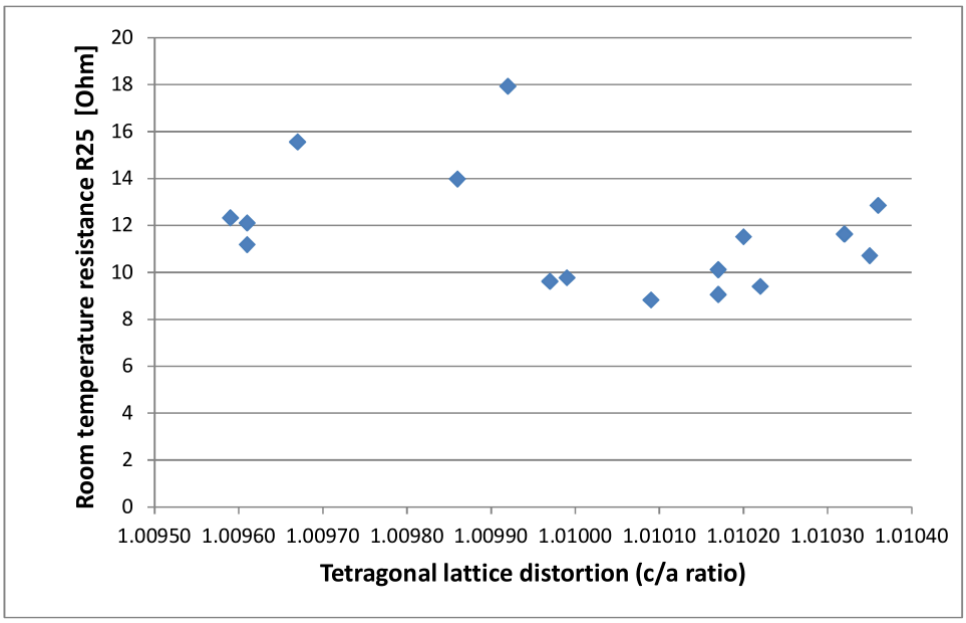

Figure 5.33: Room temperature resistance versus tetragonal lattice distortion.

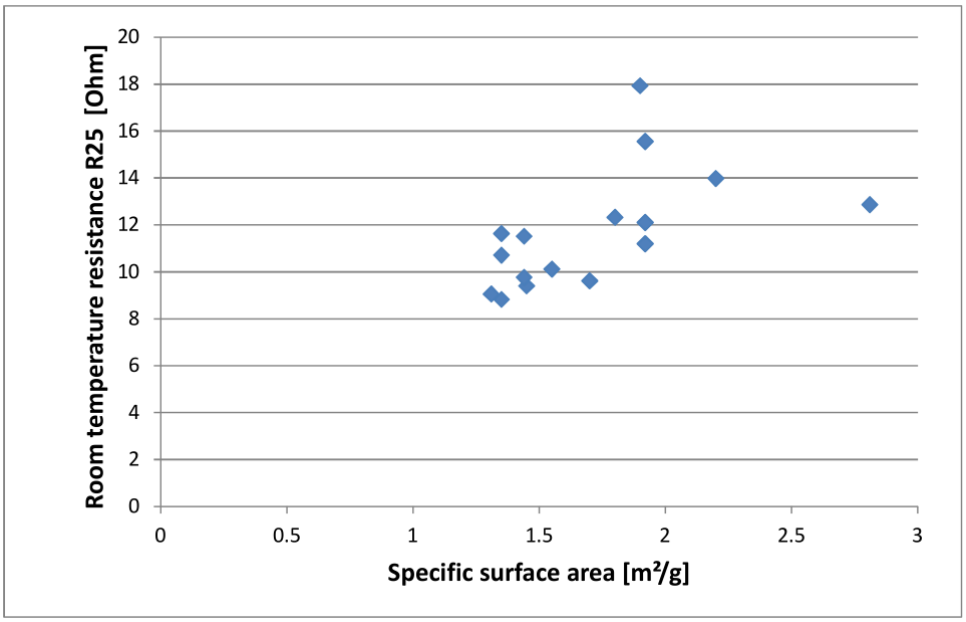

Figure 5.34: Room temperature resistance versus specific surface area.

5.5.13 Temperature of minimum resistance

The main effects diagram for the temperature of minimum resistance (T_{Rmin}) is shown in Figure 5.35. The null hypothesis analysis gives a p-value for the temperature of 1.1 %, which shows a positive influence in the plot. A lowering influence of the tube material can also be seen, but is not significant (p-value higher than 5 %).

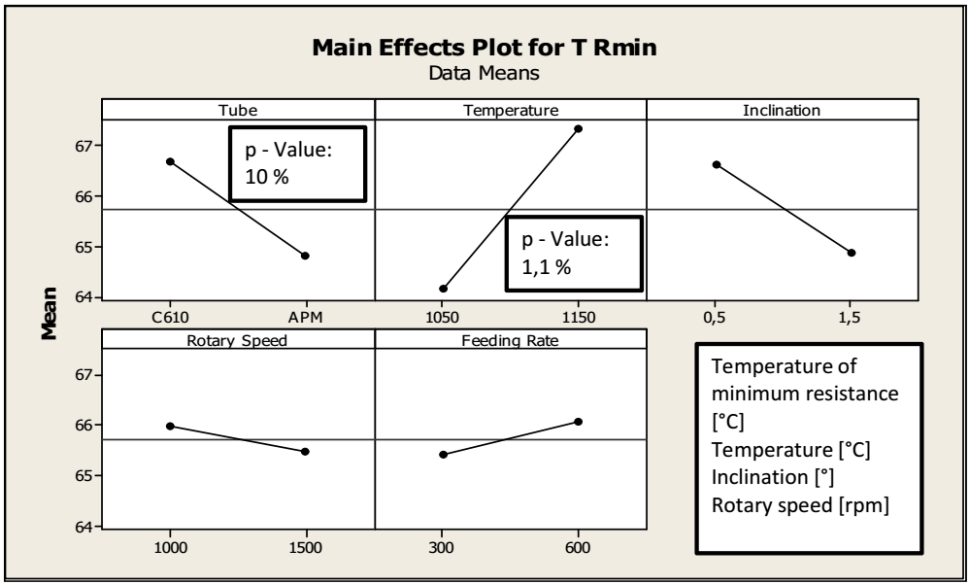

Figure 5.35: Main effects plot for temperature of minimal electrical resistance (T Rmin) in °C.

The plot in Figure 5.36 shows various slight interactions for almost all parameters. These should be interpreted with care as temperature characteristics are measured in 5 °C steps and the values in the interaction plot are mean values of only 4 experiments (see subsection 5.5.1 and Table 5.2).

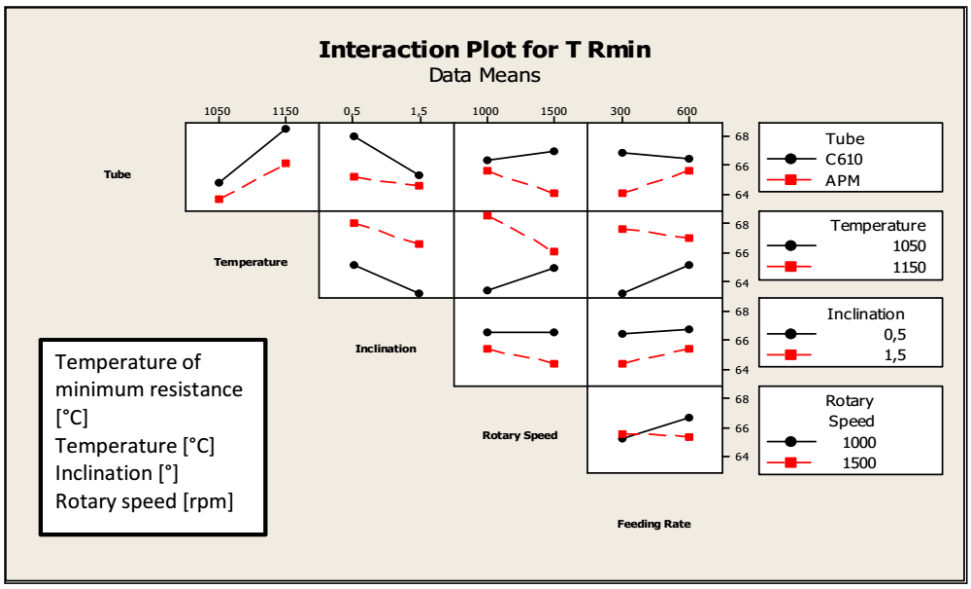

Figure 5.36: Interaction plot for temperature of minimal electrical resistance (T Rmin) in °C.

5.5.14 Reference temperature

The main effects plot for reference temperature (T_{ref}) is shown in Figure 5.37. It shows an increase of T_{ref} with calcination temperature (T_{cal}), which has a p-value of 2.5 %. A significant influence (p-value of 4.4 %) of tube material can also be seen.

The plot in Figure 5.38 shows various slight interactions for almost all parameters. These should be interpreted with care as temperature characteristics are measured in 5 °C steps and the values in the interaction plot are mean values of only 4 experiments (see subsection 5.5.1 and Table 5.2).

Figure 5.39 shows that higher room temperature resistance (R_{25}) corresponds to lower T_{ref}. (Note: R_{25} should not be confused with R25*) R_{25} is measured after the first sintering and T_{ref} results from the resistance - temperature measurement after final sintering (see section 4.8).

It was found that higher SSA values relate to a lower T_{ref}, which is shown in Figure 5.40.

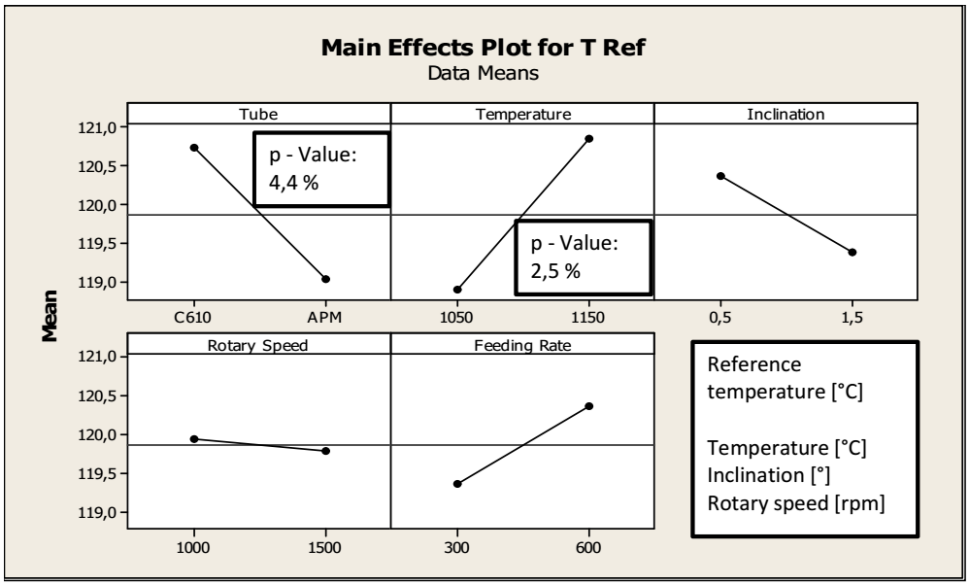

Figure 5.37: Main effects plot for reference temperature (T Ref) in °C.

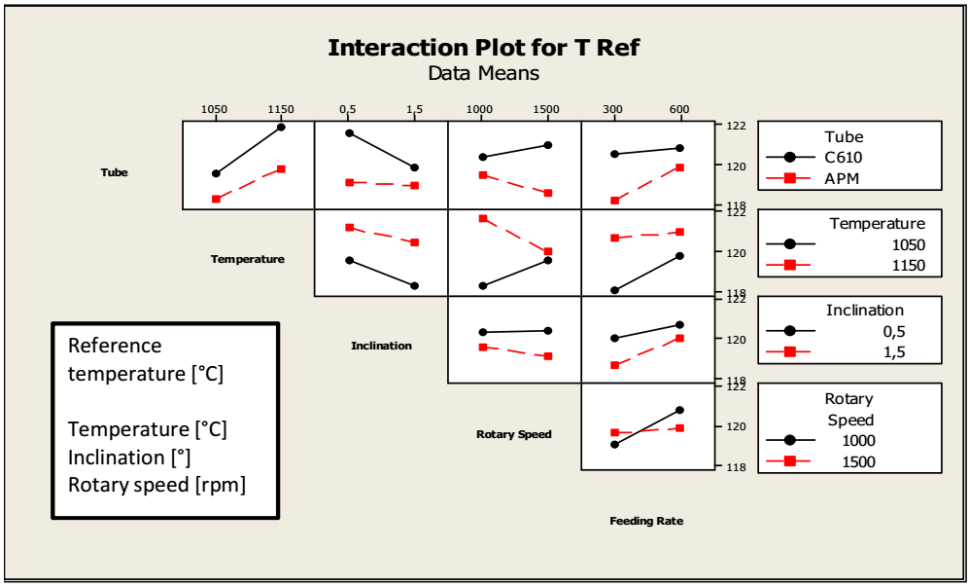

Figure 5.38: Interaction plot for reference temperature (T Ref) in °C.

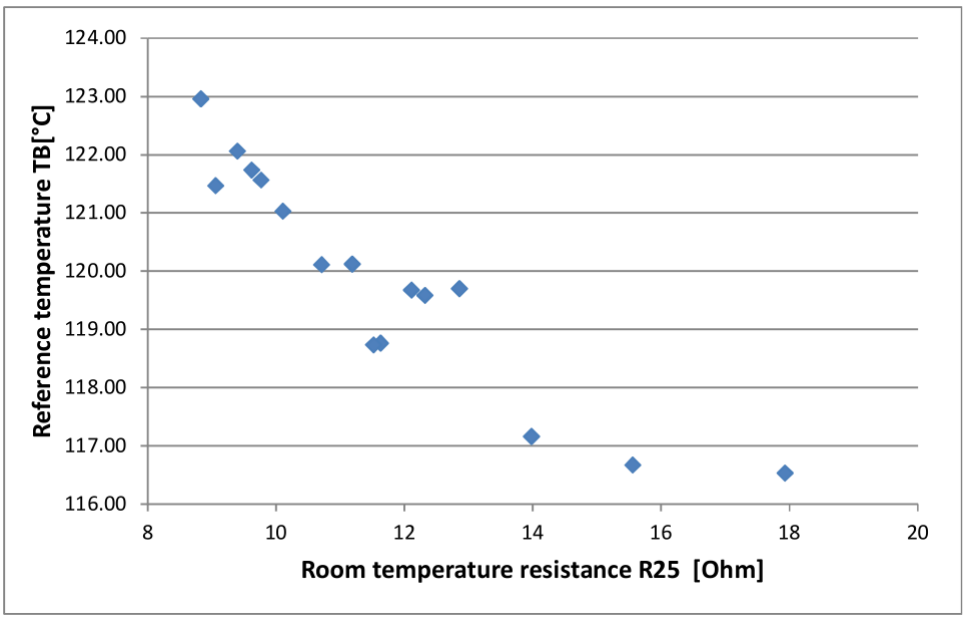

Figure 5.39: Correlation of reference temperature with room temperature resistance.

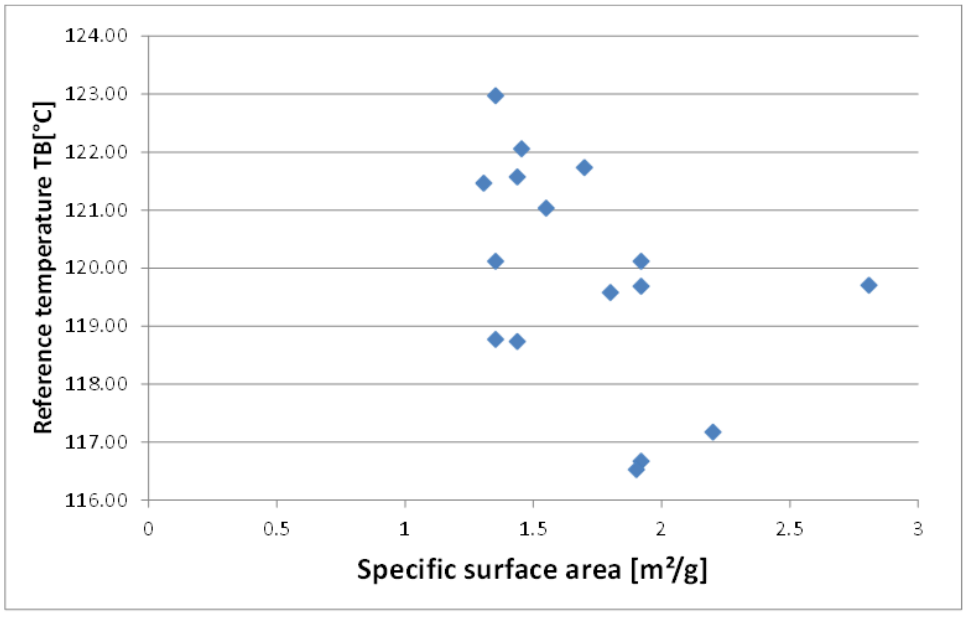

Figure 5.40: Correlation of reference temperature with specific surface area.

5.6 Temperature measurement inside tube

All given temperature settings refer to values measured outside the tube at the indirect heating elements.
A measurement of temperature (T) inside the tube at different positions for setting 1050 °C can be found in Figure 5.41. Starting from the filling mechanism, T rises and drops at the position of a ventilator.

A minimum offset of 33 °C was found between the setting of T on the control panel and actual T inside the tube. The length with offset less than 50 °C measures about 60 cm. (The heated length is 100 cm)

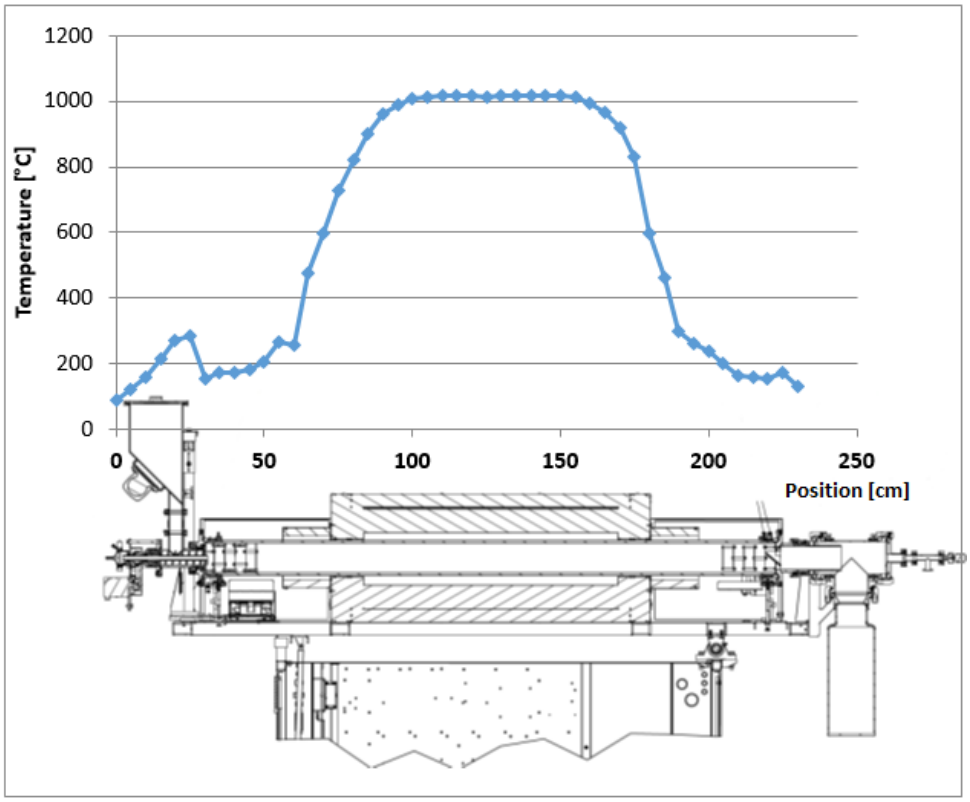

Figure 5.41: Temperature measurement inside tube at different positions for setting of 1050 °C. A schematic drawing of the rotary tube kiln is added for easier interpretation.

6 Summary and conclusion

All measurement data can be found in a separate appendix book.

6.1 Moisture content

The raw material is mixed in a wet process, filtered and dried for a defined time, but not to a defined level of moisture content (MC). Therefore material with varying MC was used for calcination experiments.

In section 5.3 it was found that the moisture content of the raw material has a great influence on the calcination process in the rotary tube kiln when no control of atmosphere is installed. The room temperature resistance R_{25} showed a factor three higher value than expected, which is out of limits.

While conducting the experiment condensing water was observed at the outlet end of the rotary tube kiln. It can be assumed that due to an opening allowing only limited amounts of gas to exit, moisture evaporating from the raw material is trapped inside the tube and results in very high humidity.

This is not observed for the pusher kiln process, where saggers are heated for about 20 h and moisture content plays only a minor role in the calcination process. The calcination time in the rotary tube kiln is about 20 min (measured from begin of filling to start of continuous output). Therefore material cannot be dried in the used set-up.

Opening one end of the tube or actively pumping gas out of the tube could improve the processability of moisture containing material.

Experiments conducted with raw material moisture content of less than 0.3 % did not show condensing water. Future experiments could be conducted using a suction at the outlet of the kiln to avoid concentration of moisture. Another solution is to dry the raw material before calcination.

6.2 Determination of experimental parameters

The first step of this work was to determine process parameters for the rotary tube kiln, which can reproduce the features (el. behaviour) of the (standard) calcination process using the pusher kiln.

It was found that the calcination temperature (T_{cal}) has the greatest influence on most of the properties. This is mainly caused by the dependence of phase composition on T_{cal} as proposed in Figure 3.2 (note that this figure shows the situation for lead-free material) and by the growth or closure of pores as shown in Figure 3.3.

Suitable parameters were found for (lead-containing) EB271 material but could not be found for lead-free EB311 (see deviations from reference in Figure 5.8).

The parameters for EB271, which produce a stable product (repetition and long-term experiments) and which are in accordance with reference values (section 5.2) turned out to be the following:

- Tube: APM
- Temperature: 1100 °C
- Inclination: 1.0°
- Rotary speed: 1300 rpm
- Feeding rate: 400 rpm

6.3 Stability of SSA and c/a ratio

The time stability of tetragonal lattice distortion (c/a ratio) and specific surface area (SSA) was studied in subsection 5.2.2.

The stability measurements of the tetragonal lattice distortion shows that the standard deviation (Std-dev) for repetition of an experiment is higher than the single measurement uncertainty. Therefore this higher value (0.00045) has to be taken into account when evaluating dependencies, e.g. in Figure 5.33 when R_{25} is considered in dependence on c/a ratio.

The stability of the specific surface area (SSA) is shown in Figure 5.10b. The Std-dev of repeated experiments ($0.07\,m^2\,g^{-1}$) is lower than the uncertainty of a single measurement. This qualifies SSA for use in process control.

6.4 Impurities and tube passivation

The amount of impurities induced by using the metal alloy tube has been studied. After 20 min of process time the impurities reach an acceptable level and a passivation of the tube for further processing can be assumed (Figure 5.11). Due to this fact the material of the first 20 min of every experiment was discarded.

6.5 Temperature profile inside tube

All given temperature settings refer to values measured at the indirect heating elements (outside of the tube). The temperature profile inside the tube can be found in Figure 5.41. A minimum offset of 33 °C was found. The length with offset less than 50 °C measures about 60 cm.

6.6 Design of experiments

A statistical driven plan for conducting experiments was designed and settings can be found in Table 5.2. It is a half factored plan (2^{5-1} experiments) and is used to determine main effects as well as second order interactions.

An overview of measured characteristics of process, powder and electric properties with reference to figures is shown in the following Table 6.1.
Table 6.2 shows an overview of the influences of process parameters on these properties.

Table 6.1: Table with references to the design of experiment main effect and interaction plots as well as correlations with the specific surface area.

Measured Property	**Main effects**	**Interaction**	**Correlation to SSA**
Troughput	Figure 5.12		
Tetragonal lattice distortion	Figure 5.14	Figure 5.15	
Specific surface area	Figure 5.16	Figure 5.17	
Apparent density	Figure 5.18		
Tapped density	Figure 5.20		
Angle of repose	Figure 5.21		
Maximum pressing power	Figure 5.22		Figure 5.23
Resilience radial	Figure 5.24		Figure 5.26
Resilience axial	Figure 5.25		
Cohesion	Figure 5.27		
Green strength radial	Figure 5.28		Figure 5.30
Green strength axial	Figure 5.29		Figure 5.30
Room temperature resistance (R25)	Figure 5.31	Figure 5.32	Figure 5.34
Temperature of minimum resistance (TRmin)	Figure 5.35	Figure 5.36	
Reference temperature (Tb)	Figure 5.37	Figure 5.38	Figure 5.40

Most interaction plots shows some weak interactions. Nevertheless it is recommended

to repeat the design of experiments series before the evaluation of interactions because mean values in these plots are calculated from only 4 experiments. With a second run of the series the data of 8 experiments would be available.

6.6.1 Specific surface area

Figure 5.16 shows that the calcination temperature directly influences the specific surface area of the powder. A higher temperature causes the closure of pores and leads to a lower surface area.
Some powder/green body properties (pressing power, resilience, green strength) and R_{25} show a correlation with the specific surface area (see Table 6.1 and Table 6.2). This may be due to the pores (directly related to SSA) in the powder/green body/final PTC, which strongly influence those properties.

This fact is very useful for process control as SSA can qualify the calcination and also be used as a target value to control properties.

6.6.2 Maximum pressing power

The maximum pressing power is significantly influenced by the calcination temperature (lowering) and tube inclination (rising). It is a very important factor in PTC production as high pressures can be hard to control exactly and some samples almost reached the maximum possible pressure limited by the press. Increasing temperature lowers the needed pressing power and can be used to achieve desired (lower) values.

Pores in the powder are reduced during calcination (see SSA above). This process depends on temperature and time spent (influenced by tube inclination) inside the tube. The pores might influence the internal friction of particles and cause the need for higher pressing power. Therefore a lower SSA (higher T_{cal}) correlates to lower pressing power as can be seen in Figure 5.23.

6.6.3 Resilience

The resilience is the change of size of a green body after ejection from the shaping tool. It can cause micro-cracks in parts and influences durability of PTCs. It is therefore important to achieve a proper resilience as well as to be able to influence it. The main effects plot (Figure 5.24) shows temperature as the only significant factor. This is caused by the pores size (see above, SSA), and is shown in the SSA correlation plot (Figure 5.26).

6.6.4 Green strength

The strength of green bodies is important for the processability/handling. This strength is governed to a great extent by T_{cal} (see Figure 5.28). A higher temperature (which corresponds to lower SSA) decreases the green strengths. This relation with SSA is shown in Figure 5.30.

6.6.5 Room temperature resistance (R25)

The temperature effect on R_{25} (lower for high T) is due to the formation of different phases as proposed in Figure 3.2. It should be noted that the literature describes the situation for lead free material and a lower calcination temperature is needed when adding lead. Other parameters can also be expected to influence this phase composition, but only in a limited way.

The specific surface area can be used to quantify the calcination progress (see above, SSA). The progressing calcination lowers SSA and also corresponds to lower R_{25}, which is shown in Figure 5.34.

Lower reference temperatures (T_{ref}) are observed for higher R_{25} values, which can be seen in Figure 5.39. The two values are determined at different steps of the production

(see section 4.8). Therefore the dependency can be very useful to predict if the resistance-temperature behaviour will be within limits, before measuring the whole temperature range.

6.6.6 Reference and minimum resistance temperature (Tb and TRmin)

The reference temperature (T_{Ref}) and the temperature of minimum resistance (T_{Rmin}) show similar DoEx plots (Table 6.1) due to their definition (see subsection 2.2.1). Both show a significant (raising) dependence on T_{cal}. The tube material shows an influence on T_{Ref} (p-value of 4.4 %). This should be seen as a significant influence, but is not easily explainable. Therefore further investigation by repeating the design of experiments series is recommended.

Lower T_{Ref} values can be related to higher SSA as shown in Figure 5.40.

6.7 Conclusion

The significant influences that can be concluded from the design of experiments are shown in Table 6.2. It contains all quantities (powder, green body, process and electric) and shows the direction of the influence of process parameters as well as of SSA and R_{25}.

The temperature was found to be the main influencing factor for many quantities. Some of these show a correlation with specific surface area (SSA). This fact together with the stability (subsection 5.2.2) allows to use the SSA as a measure of calcination progress and a means of process control.
E.g. if a high SSA is measured a high pressing power can be expected (Figure 5.23). The pressing power (and SSA) can then be decreased by a well known value by increasing the calcination temperature (Figure 5.22). A final measurement of SSA confirms the successful process control.

Table 6.2: Schematic influences of process parameters as well as specific surface area and room temperature resistance on all determined quantities (process, electric, powder, green body).

Parameter → / Quantity ↓	Tube - material	Temp.	Inclin.	Tube - speed	Feeding - rate	SSA	R25
Dwell time			↓	↓			
Filling grade (%)			↓		↑		
Throughput			↑	↑	↑		
R25 (Ohm)		↓				↑	
T Rmin		↑				↓	
T Ref	↓ (APM)	↑				↓	↓
Ratio c/a		↑					
SSA (m^2/g)		↓					
Apparent density		↑				↓	
Tamped density		↑					
Repose angle	↑ (APM)						
Max. press power		↓	↑			↑	
Resilience radial		↓				↑	
Resilience axial		↓					
Cohesion							
Green strength axial		↓				↑	
Green strength radial		↓				↑	

6.8 Outlook

Further investigation of the rotary tube kiln process should be done to improve process control and get more knowledge about the process behaviour.
This includes:

- Repeating the design of experiments series to gain more precise knowledge
- Repeated long term experiments, also with C610 tube
- Investigation of lead free materials
- Install suction at the outlet and try material with higher moisture content
- Testing gained knowledge with other material mixtures
- Running long term tests for the produced parts to allow official distribution to end users
- Scale-up and purchase of a kiln model with higher troughput for production

Bibliography

[1] EPCOS AG. *PTC Thermistors, General technical information*. 2016. URL: https://de.tdk.eu/tdk-de/545350/produkte/produktsuche/technische-parameter/produktkatalog/keramische-bauelemente/ptc-thermistoren/ptc-thermistoren-fuer-motorstart-anwendungen?t=ps (visited on 02/13/2017) (cit. on pp. 1, 7).

[2] Precision Ceramics. *Dimulit C610*. 2017. URL: http://www.precision-ceramics.co.uk/materials/ceramtec/dimulit-c610/ (visited on 03/09/2017) (cit. on p. 17).

[3] Rainer Hölzle. *Elektrokeramische Materialien: Grundlagen und Anwendungen ; vom 6. März bis 17. März 1995*. German. Vol. 26. Jülich: Forschungszentrum Jülich, 1995. ISBN: 9783893361465;3893361464; (cit. on pp. 5, 6, 8).

[4] Kanthal. *Kanthal APM datasheet*. 2017. URL: http://www.kanthal.com/en/products/material-datasheets/tube/kanthal-apm/ (visited on 03/09/2017) (cit. on p. 17).

[5] Wilhelm Kleppmann. *Versuchsplanung: Produkte und Prozesse optimieren*. German. 2013. ISBN: 9783446437913;3446437916; (cit. on p. 23).

[6] Almut Melzer. *Six Sigma - Kompakt und praxisnah: Prozessverbesserung effizient und erfolgreich implementieren*. German. 2015 (cit. on p. 23).

[7] A. J. Moulson and J. M. Herbert. *Electroceramics: materials, properties, applications*. English. 1., reprint. as a paperback. London [u.a.]: Chapman and Hall, 1993. ISBN: 041247360 7;9780412473609; (cit. on pp. 1, 5–10, 12, 13).

[8] Oleg D. Neikov. *Handbook of Non-Ferrous Metal Powders: Technologies and Applications*. English. GB: Elsevier Science, 2009;2008; ISBN: 1856174220;9781856174220;9781493303847;1
(cit. on p. 20).

[9] Shigeo Hayashi Sakake Tsutai Tomoki Hayashi and Zenbe-e Nakagawa. "Reaction Mechanism of BaTiO3 from Powder Compacts, BaCO3 and TiO2 and Expansion Phenomena during the Formation Process". In: *Journal of the Ceramic Society of Japan* 109 (2001) (cit. on pp. 14, 15).

[10] Karl Siebertz, David Bebber, and Thomas Hochkirchen. *Statistische Versuchsplanung: Design of Experiments (DoE)*. German. Berlin [u.a.]: Springer, 2010. ISBN: 9783642054921;3642054927; (cit. on pp. 23, 24).

[11] Edward Teller Stephen Brunauer P. H. Emmett. "Adsorption of Gases in Multimolecular Layers". In: *Journal of the American Chemical Society* 60, Nr. 2 (1938), pp. 309–319 (cit. on p. 19).

[12] William G. Truscott. *Six sigma: continual improvement for business : a practical guide*. English. 2003. ISBN: 0750657650;9780750657655; (cit. on p. 23).

[13] Roland Würschum. *Masterstudium Advanced Materials Science: Funktionswerkstoffe I, Vorlesungsskriptum*. German. 2016 (cit. on p. 6).

List of Figures